The combined effects of confining pressure, temperature, and mineralogical composition on the dynamic elastic constants of rock

Dr.-Ing. Hem Bahadur Motra

Department of Geosciences, Geomechanics and Geotechnics
Kiel University (CAU)

EGU: Tertiary Education Geosceince: 2025

Outlines

Motivation

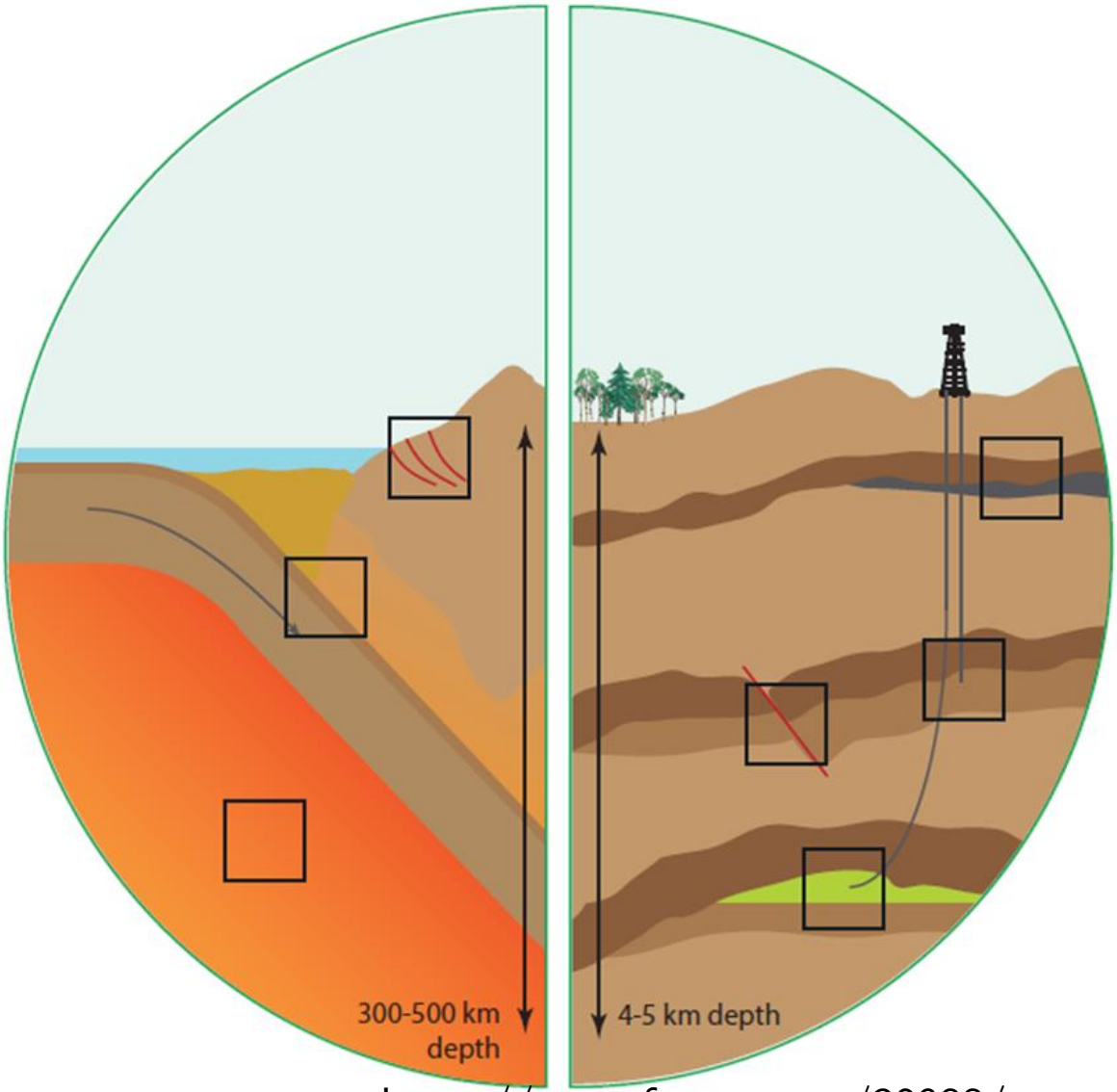

https://svs.gsfc.nasa.gov/30988/

- Geothermal exploration
- Oil/gas recovery
- CO2 storage
- Radioactive waste disposal
- Groundwater contamination
- Deep earth and solar system
- Acid mining

Main objectives of the talk

Part I

- Measurements of P- and S-wave velocities and S-wave splitting in 3 orthogonal directions
- Effect of anisotropy on tensors and petrophysical properties of rocks
- To investigate the lithological control and the effect of pressure and temperature on seismic properties of crustal rocks
- To analyse the effects of pressure, temperature ans mineralogical on elastic constants of rocks

Part II

- 3D velocity calculations based on the crystallographic preferred orientation (CPO) of major minerals

Structure of Earth

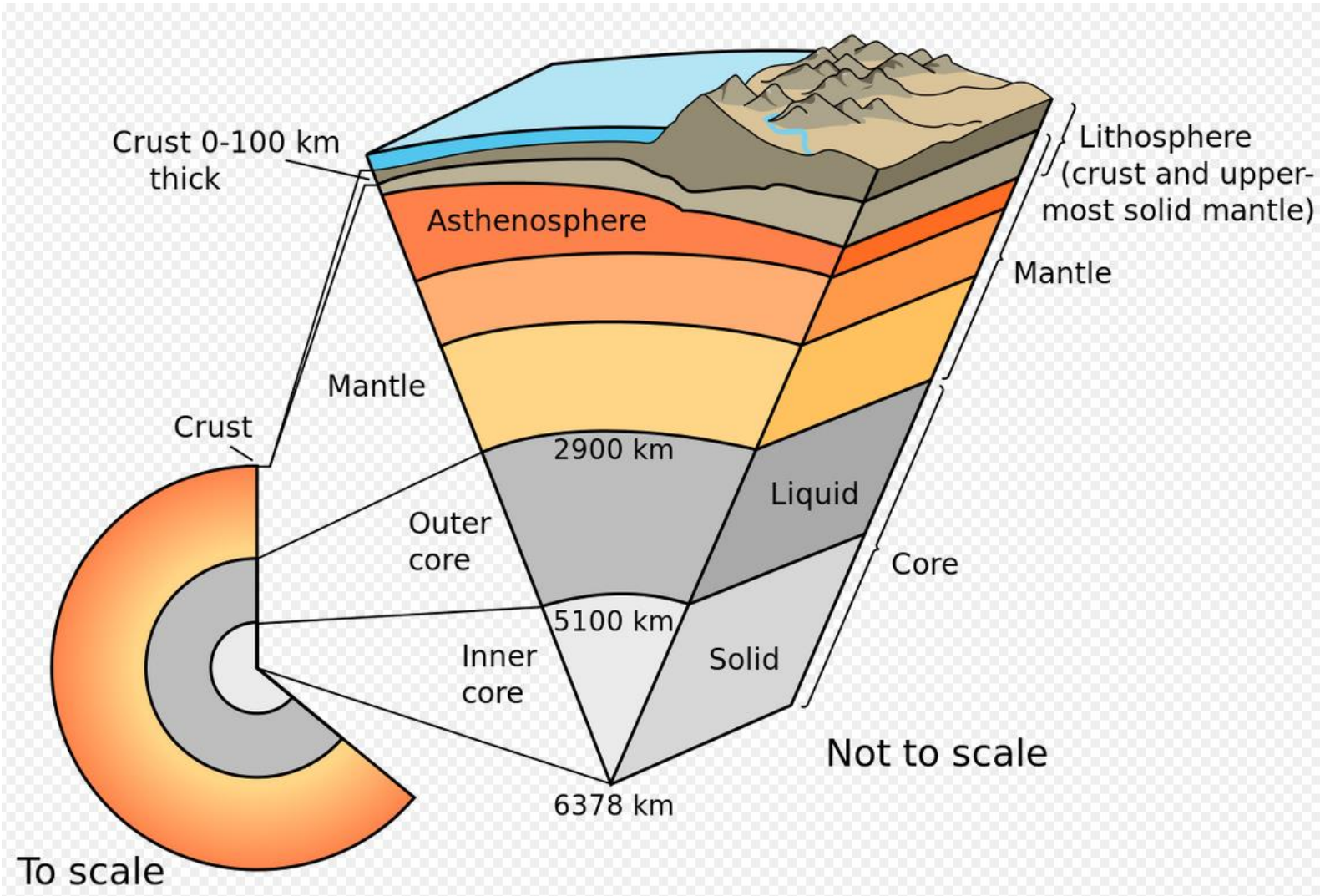

https://www.internetgeography.net/topics/structure-

Anisotropy

Definition

- Seismic anisotropy is the dependence of seismic velocity upon angle
- This definition yields both P- and S-waves

Definition

- We have to distinguish between anisotropy and heterogeneity
- Heterogeneity is the dependence of physical properties upon position
- Heterogeneity on the small scale can appear as seismic anisotropy on the large scale

Physical properties

Physical properties of rocks

- Physical properties from microstructural information (crystal orientation, volume fraction, grain shape etc.) are important for rocks
- In-situ state at high temperature and pressure for samples where the microstructure has been changed by subsequent chemical alteration (e.g. the transformation olivine to serpentine) or mechanically induced changes (e.g. fractures created by decompression)
- The effect of phase change on the physical properties can also be modeled using these methods.
- Anisotropic properties as experimental measurements in many directions necessary to fully characterize anisotropy is currently feasible for the majority of the temperature and pressure conditions

The origin of seismic anisotropy

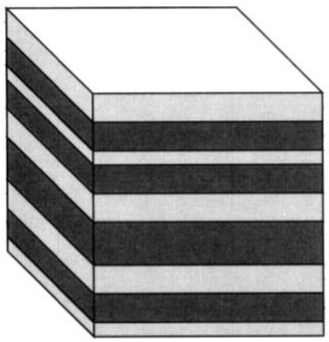

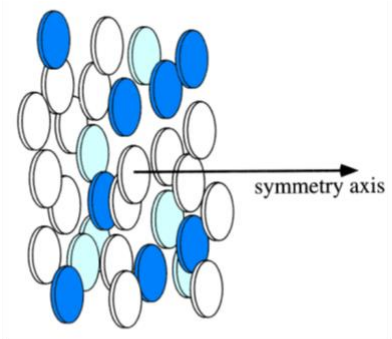

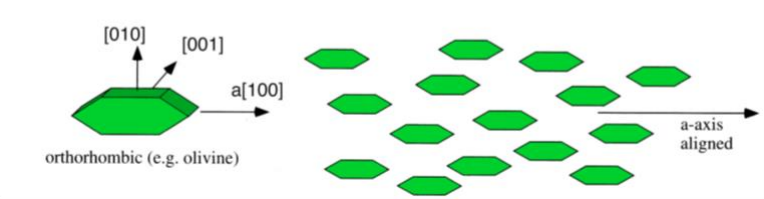

- Horizontal layering - sediments, metamorphic layering, Upper and lower crust, transition zone
- Vertically aligned cracks in the crust filled with gas, liquid or solid
- Crystal preferred orientation (CPO) in lower crust, upper mantle and inner core

3D Elasticity

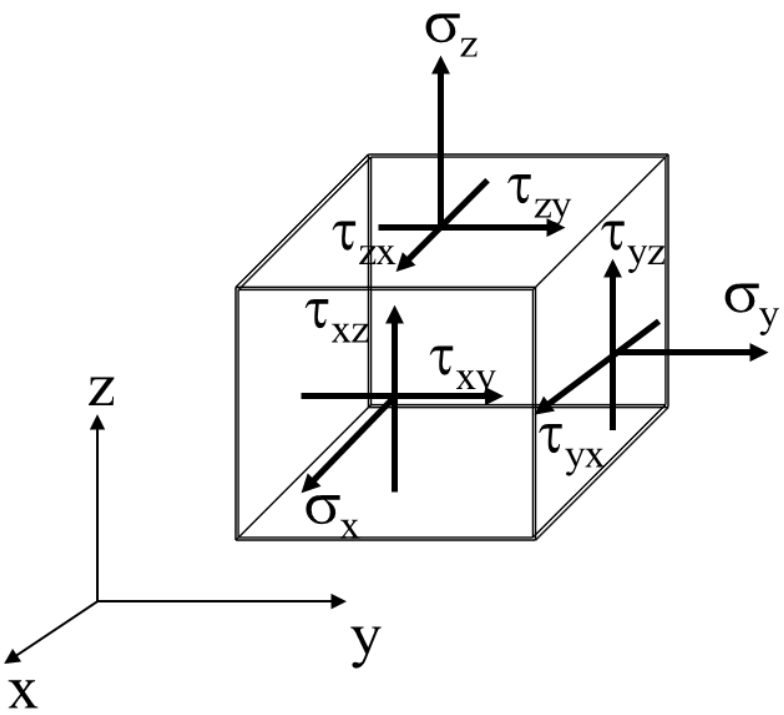

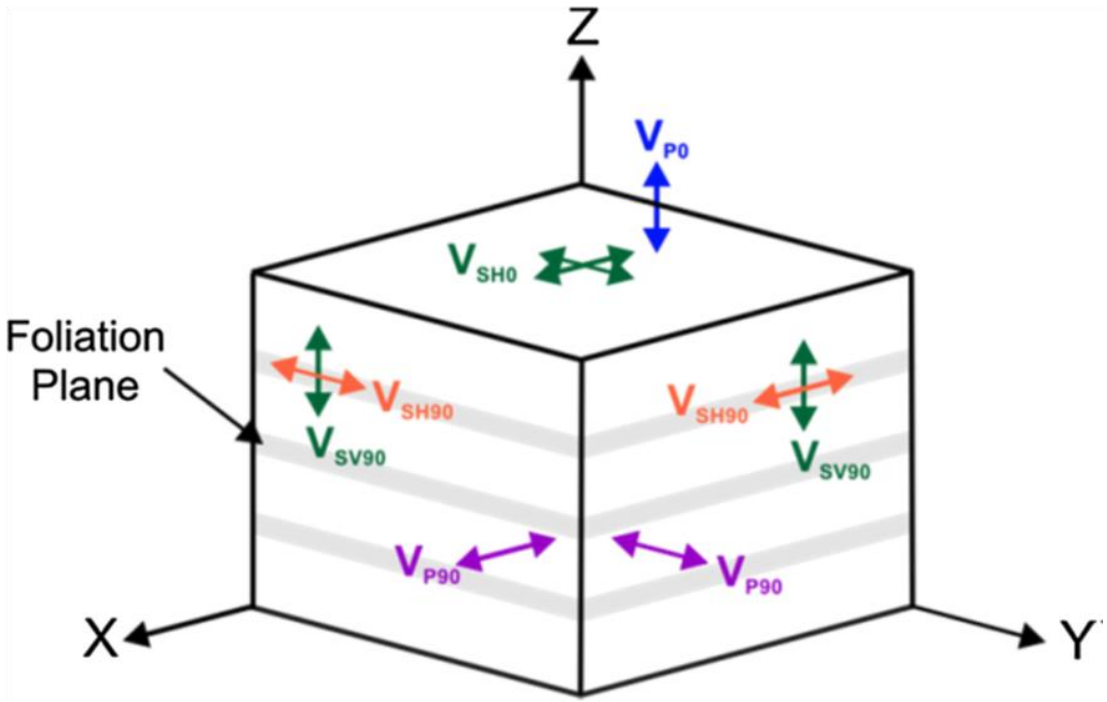

Symmetry of a transversely isotropic medium where elastic properties are rotationally symmetric about the z-axis. Arrows of the same color indicate waves propagating at the same speed while their directions indicate the wave's polarization

Elasticity tensor

- In general 3-D case, there are six components of stress and corresponding six components of strain.
- In highly anisotropic materials, any one component of stress can cause strain in all six components
- For the generalized case, Hooke's law may be expressed as:

$$\sigma_i = C_{ij}\varepsilon_j$$

$$\varepsilon_i = S_{ij}\sigma_j$$

where,
C $\rightarrow$ Stiffness (or Elastic constant)
S $\rightarrow$ Compliance

3D Elasticity

- In matrix format, the stress-strain relation showing the 36 (6 x 6) independent components of stiffness can be represented as:

$$\begin{pmatrix} \sigma_1 \\ \sigma_2 \\ \sigma_3 \\ \sigma_4 \\ \sigma_5 \\ \sigma_6 \end{pmatrix} = \begin{pmatrix} C_{11} & C_{12} & C_{13} & C_{14} & C_{15} & C_{16} \\ C_{21} & C_{22} & C_{23} & C_{24} & C_{25} & C_{26} \\ C_{31} & C_{32} & C_{33} & C_{34} & C_{35} & C_{36} \\ C_{41} & C_{42} & C_{43} & C_{44} & C_{45} & C_{46} \\ C_{51} & C_{52} & C_{53} & C_{54} & C_{55} & C_{56} \\ C_{61} & C_{62} & C_{63} & C_{64} & C_{65} & C_{66} \end{pmatrix} \begin{pmatrix} \varepsilon_1 \\ \varepsilon_2 \\ \varepsilon_3 \\ \varepsilon_4 \\ \varepsilon_5 \\ \varepsilon_6 \end{pmatrix}$$

- or in short notation, we can write

$$\sigma_i = C_{ij}\varepsilon_j$$

$$\varepsilon_i =_{ij} \sigma_j$$

VTI (Vertically Transverse Isotropy)

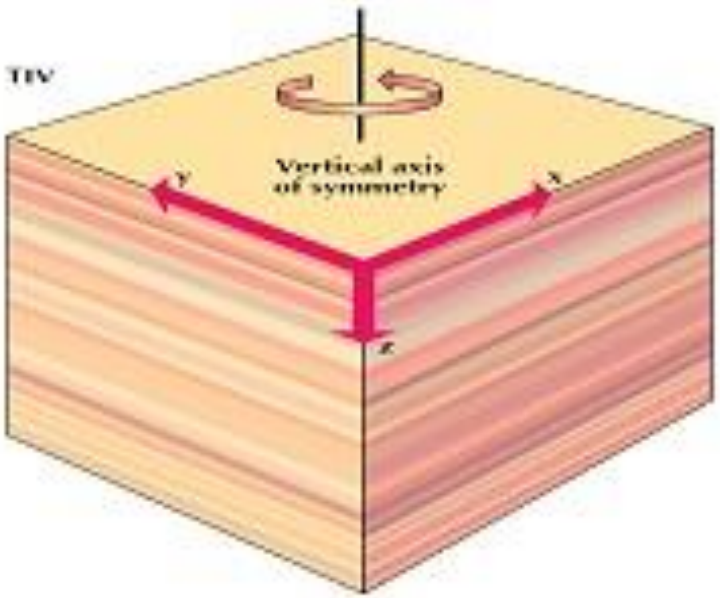

Schmitt (2015)

$$\begin{pmatrix} C_{11} & C_{11}-2C_{66} & C_{13} & 0 & 0 & 0 \\ C_{11}-2C_{66} & C_{11} & C_{13} & 0 & 0 & 0 \\ 0 & 0 & C_{33} & 0 & 0 & 0 \\ 0 & 0 & 0 & C_{44} & 0 & 0 \\ 0 & 0 & 0 & 0 & C_{44} & 0 \\ 0 & 0 & 0 & 0 & 0 & C_{66} \end{pmatrix}$$

HTI (Horizontally Transverse Isotropy)

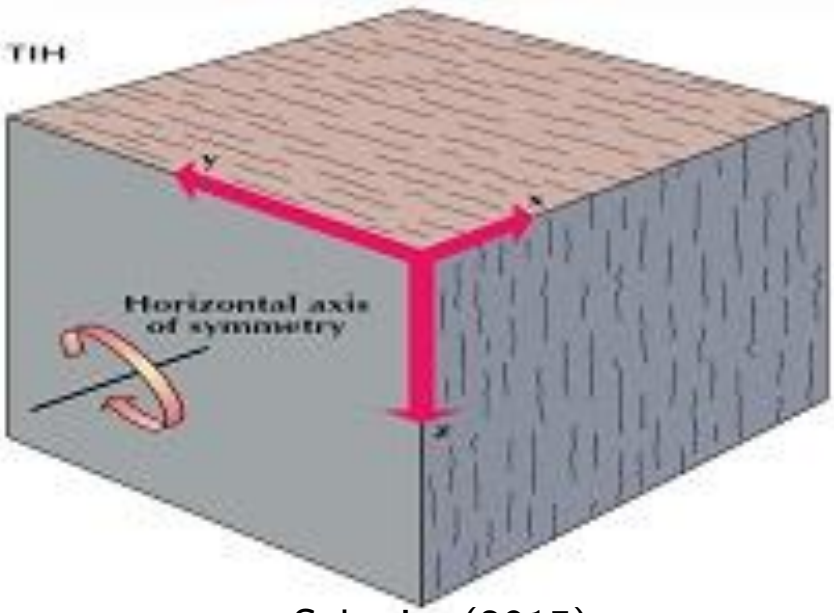

Schmitt (2015)

$$\begin{pmatrix} C_{11} & C_{13} & C_{13} & 0 & 0 & 0 \\ C_{13} & C_{33} & C_{13}-2C_{44} & 0 & 0 & 0 \\ C_{13} & C_{13}-2C_{44} & C_{33} & 0 & 0 & 0 \\ 0 & 0 & 0 & C_{44} & 0 & 0 \\ 0 & 0 & 0 & 0 & C_{44} & 0 \\ 0 & 0 & 0 & 0 & 0 & C_{66} \end{pmatrix}$$

Orthogonal Fracture Sets

https://www.alamy.com/stock-photo/fractured-rock.html?sortBy=relevant

Orthorhombic Model

$$\begin{pmatrix} C_{11} & C_{12} & C_{13} & 0 & 0 & 0 \\ C_{12} & C_{22} & C_{23} & 0 & 0 & 0 \\ C_{13} & C_{23} & C_{33} & 0 & 0 & 0 \\ 0 & 0 & 0 & C_{44} & 0 & 0 \\ 0 & 0 & 0 & 0 & C_{55} & 0 \\ 0 & 0 & 0 & 0 & 0 & C_{66} \end{pmatrix}$$

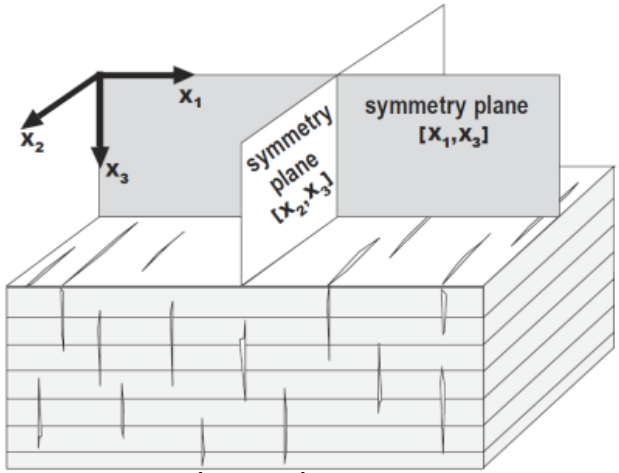

Tsvankin, (2001)

C_{ij} Effect of Crystal Symmetry

Seismic anisotropy symmetries

Triclinic (21 constants)

$$\begin{pmatrix} C_{11} & C_{12} & C_{13} & C_{14} & C_{15} & C_{16} \\ - & C_{22} & C_{23} & C_{24} & C_{25} & C_{26} \\ - & - & C_{33} & C_{34} & C_{35} & C_{36} \\ - & - & - & C_{44} & C_{45} & C_{46} \\ - & - & - & - & C_{55} & C_{56} \\ - & - & - & - & - & C_{66} \end{pmatrix}$$

Monoclinc (13 constants)

$$\begin{pmatrix} C_{11} & C_{12} & C_{13} & 0 & C_{15} & 0 \\ - & C_{22} & C_{23} & 0 & C_{25} & 0 \\ - & - & C_{33} & 0 & C_{35} & 0 \\ - & - & - & C_{44} & 0 & C_{46} \\ - & - & - & - & C_{55} & 0 \\ - & - & - & - & - & C_{66} \end{pmatrix}$$

Orthorhombic (9 constants)

$$\begin{pmatrix} C_{11} & C_{12} & C_{13} & 0 & 0 & 0 \\ - & C_{22} & C_{23} & 0 & 0 & 0 \\ - & - & C_{33} & 0 & 0 & 0 \\ - & - & - & C_{44} & 0 & 0 \\ - & - & - & - & C_{55} & 0 \\ - & - & - & - & - & C_{66} \end{pmatrix}$$

Trigonal (7 constants)

$$\begin{pmatrix} C_{11} & C_{12} & C_{13} & C_{14} & C_{15} & 0 \\ - & C_{11} & C_{13} & -C_{14} & -C_{15} & 0 \\ - & - & C_{33} & 0 & 0 & 0 \\ - & - & - & C_{44} & 0 & -C_{15} \\ - & - & - & - & C_{44} & C_{14} \\ - & - & - & - & - & C_{66} \end{pmatrix}$$

Trigonal (6 constants)

$$\begin{pmatrix} C_{11} & C_{12} & C_{13} & C_{14} & 0 & 0 \\ - & C_{11} & C_{13} & -C_{14} & 0 & 0 \\ - & - & C_{33} & 0 & 0 & 0 \\ - & - & - & C_{44} & 0 & 0 \\ - & - & - & - & C_{44} & 0 \\ - & - & - & - & - & C_{66} \end{pmatrix}$$

Hexagonal (5 constants)

$$\begin{pmatrix} C_{11} & C_{12} & C_{13} & 0 & 0 & 0 \\ - & C_{11} & C_{13} & 0 & 0 & 0 \\ - & - & C_{33} & 0 & 0 & 0 \\ - & - & - & C_{44} & 0 & 0 \\ - & - & - & - & C_{44} & 0 \\ - & - & - & - & - & C_{66} \end{pmatrix}$$

Tetragonal (7 constants)

$$\begin{pmatrix} C_{11} & C_{12} & C_{13} & 0 & 0 & C_{16} \\ - & C_{11} & C_{13} & 0 & 0 & -C_{16} \\ - & - & C_{33} & 0 & 0 & 0 \\ - & - & - & C_{44} & 0 & 0 \\ - & - & - & - & C_{44} & 0 \\ - & - & - & - & - & C_{66} \end{pmatrix}$$

Tetragonal (6 constants)

$$\begin{pmatrix} C_{11} & C_{12} & C_{13} & 0 & 0 & 0 \\ - & C_{11} & C_{13} & 0 & 0 & 0 \\ - & - & C_{33} & 0 & 0 & 0 \\ - & - & - & C_{44} & 0 & 0 \\ - & - & - & - & C_{44} & 0 \\ - & - & - & - & - & C_{66} \end{pmatrix}$$

Cubic (3 constants)

$$\begin{pmatrix} C_{11} & C_{12} & C_{12} & 0 & 0 & 0 \\ - & C_{11} & C_{12} & 0 & 0 & 0 \\ - & - & C_{11} & 0 & 0 & 0 \\ - & - & - & C_{44} & 0 & 0 \\ - & - & - & - & C_{44} & 0 \\ - & - & - & - & - & C_{44} \end{pmatrix}$$

Velocity and elastic constants

- Elastic constants

$$C_{11} = \rho v_{xx}^2, C_{22} = \rho v_{yy}^2, C_{33} = \rho v_{zz}^2$$

$$C_{44} = \rho v_{yz}^2 = \rho v_{zy}^2, C_{55} = \rho v_{xz}^2 = \rho v_{zx}^2, C_{66} = \rho v_{xy}^2 = \rho v_{yx}^2$$

$$C_{12} = [C_{66}^2 - C_{11}C_{22} + C_{66}(C_{11} + C_{22}) + 4\rho^2 v_{66}^4(45^\circ)$$
$$-2\rho v_{66}^2(45^\circ)(C_{11} + C_{22} + 2C_{66})]^{0.5} - C_{66}$$

- C_{13} and C_{23} calculate in similar way
- Thomsen's anisotropic parameters

$$\varepsilon = \frac{C_{11} - C_{33}}{2C_{33}}, \gamma = \frac{C_{66} - C_{44}}{2C_{44}}$$

$$\delta = \frac{(C_{13} + C_{44}) - (C_{33} - C_{44})}{2C_{33}(C_{33} - C_{44})}$$

Coefficients of the symmetric matrix of the fourth-order elasticity tensor

$C_{11} = c_{1111} = c_{xxxx}$	$C_{12} = c_{1122} = c_{xxyy}$	$C_{13} = c_{1133} = c_{xxzz}$	$C_{14} = c_{1123} = c_{xxyz}$	$C_{15} = c_{1131} = c_{xxzx}$	$C_{16} = c_{1112} = c_{xxxy}$
	$C_{22} = c_{2222} = c_{yyyy}$	$C_{23} = c_{2233} = c_{yyzz}$	$C_{24} = c_{2223} = c_{yyyz}$	$C_{25} = c_{2231} = c_{yyzx}$	$C_{26} = c_{2212} = c_{yyxy}$
		$C_{33} = c_{3333} = c_{zzzz}$	$C_{34} = c_{3323} = c_{zzyz}$	$C_{35} = c_{3331} = c_{zzzx}$	$C_{36} = c_{3312} = c_{zzxy}$
			$C_{44} = c_{2323} = c_{yzyz}$	$C_{45} = c_{2331} = c_{yzzx}$	$C_{46} = c_{2312} = c_{yzxy}$
				$C_{55} = c_{3131} = c_{yxzx}$	$C_{56} = c_{3112} = c_{zxxy}$
					$C_{66} = c_{1212} = c_{xyxy}$

symmetric matrix

Characteristics of crustal and mantle rocks

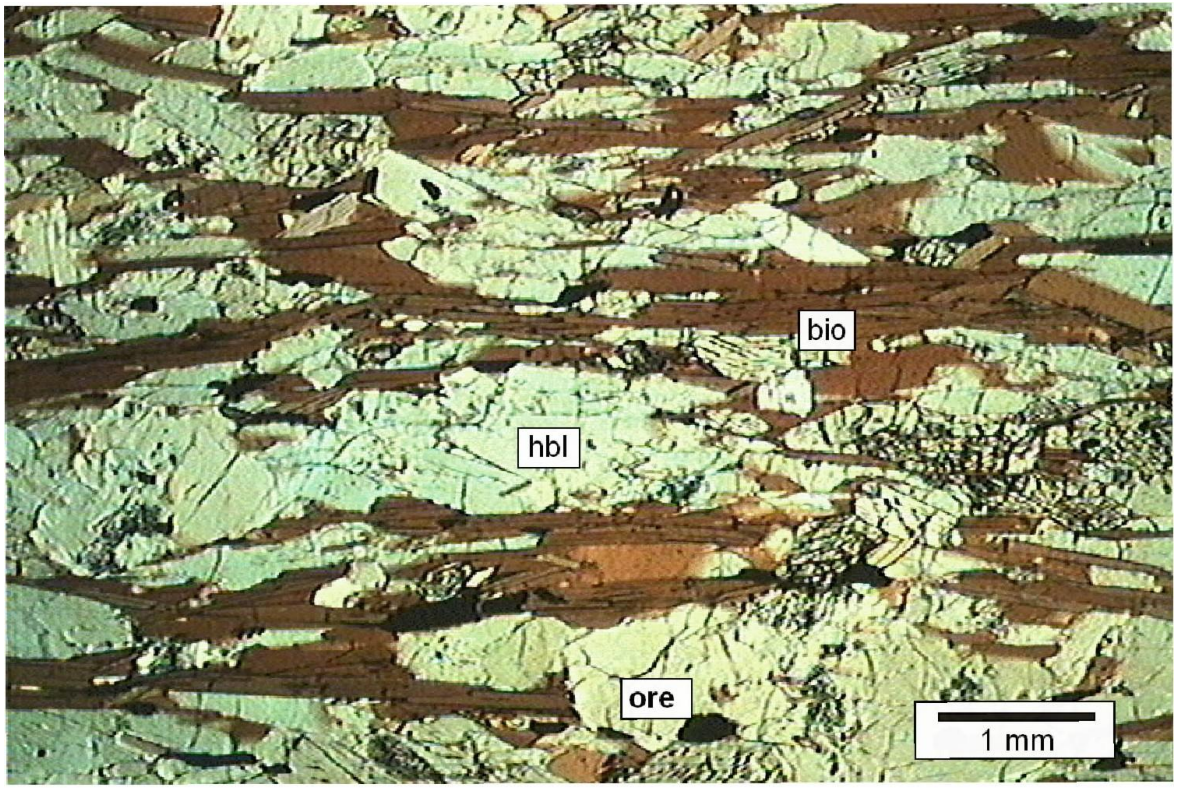

Thin section: Bio-Hbl-gneiss SD-3 36058
Kola-super deep, depth: 9571 m

- Polyphase materials
- Low-symmetry minerals with different chemical and physical properties
- Different grain shapes and grain sizes
- Cracks and pores, sometimes filled with fluids or melts
- Anisotropy of the fabric

Factors controlling

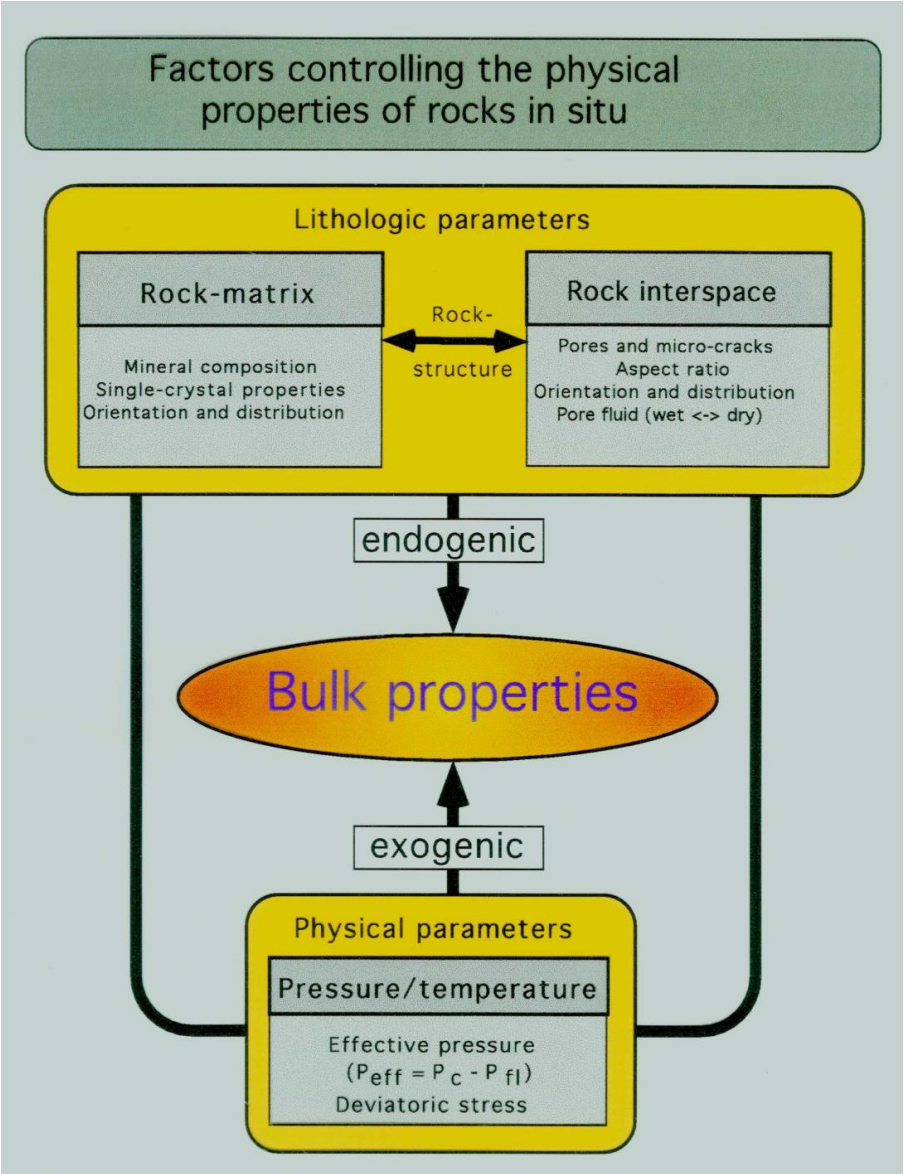

Key questions

Key questions with respect to the in situ properties

- the role of lithology (mineral composition of the rocks)
- the role of microstructural and textural characteristics (rock fabric + microcracks)
- the role of intergranular fluids
- the role of the actual stress field

Geometries

- Experimental determination of elastic wave velocities and anisotropy

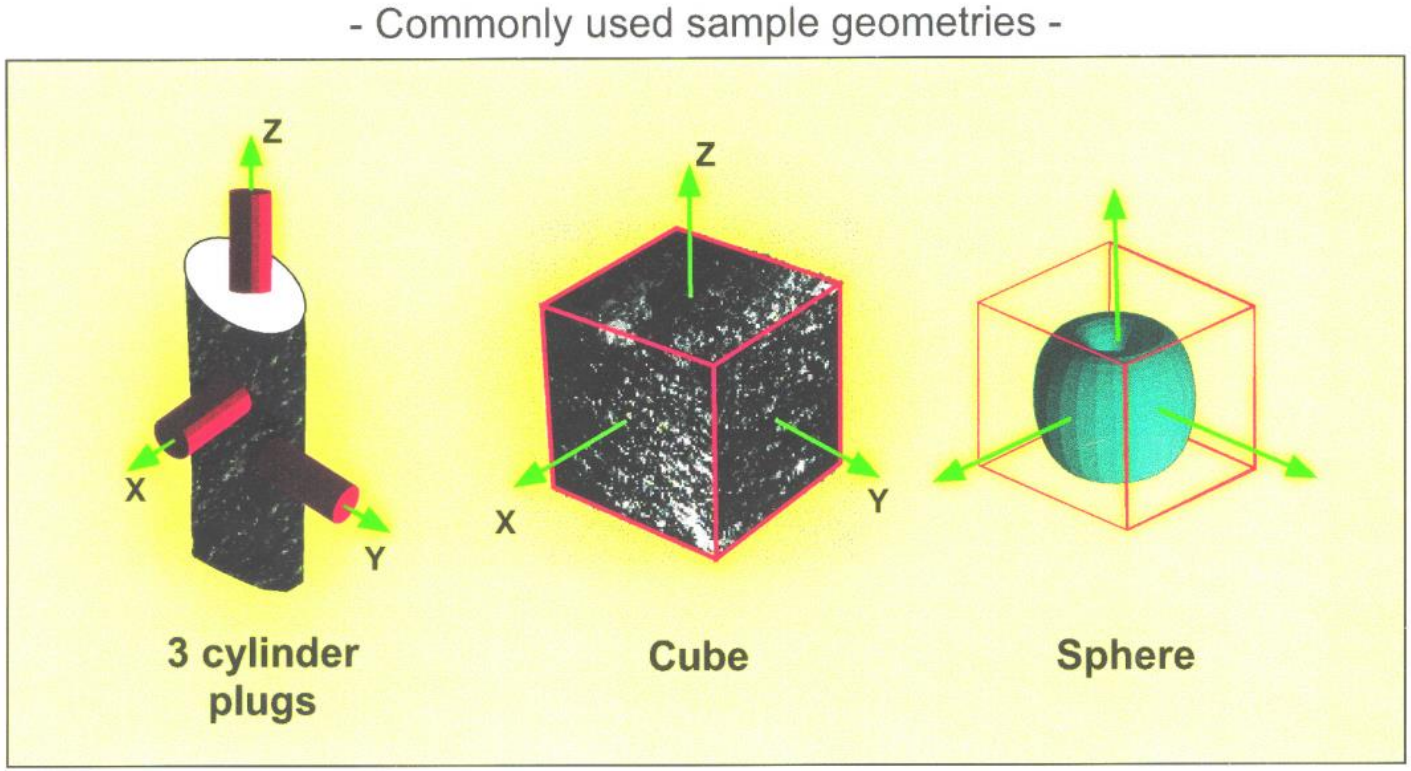

- Jacketed cylindrical samples in internally heated fluid or gas apparatus. Measurement of Vp and Vs in one direction, ⇒ truely hydrostatic pressure
- Unjacketed cubes in an externally heated multi-anvil apparatus. Simultaneous measurements of Vp and Vs in X, Y, Z. Volume (density) change ⇒ Near-hydrostatic pressure.
- Jacketed spherical samples in a fluid-filled pressure vessel. Measurement of the spatial distribution of Vp at room temperature, ⇒ truely hydrostatic pressure

Sample and sample reference system

Sample reference system

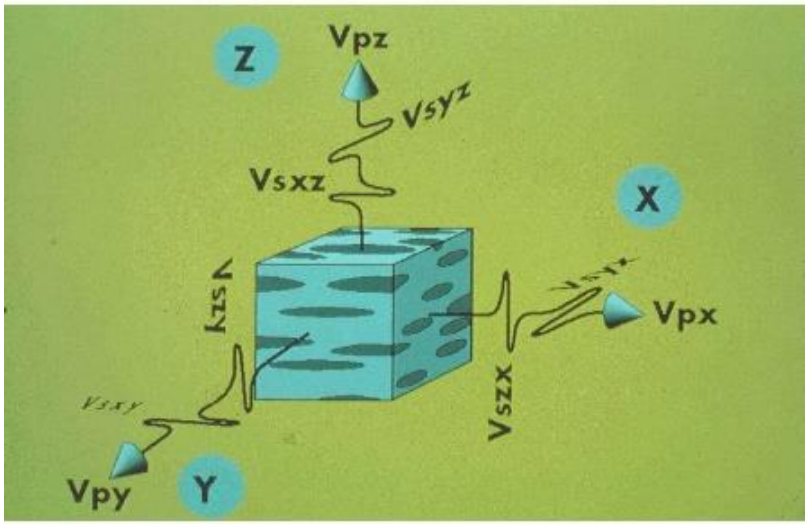

x = parallel to lineation, parallel to foliation
y = normal to lineation, parallel to foliation
z = normal to foliation

Sample, cube of 43 mm

Sample reference system

Sample and sample reference system

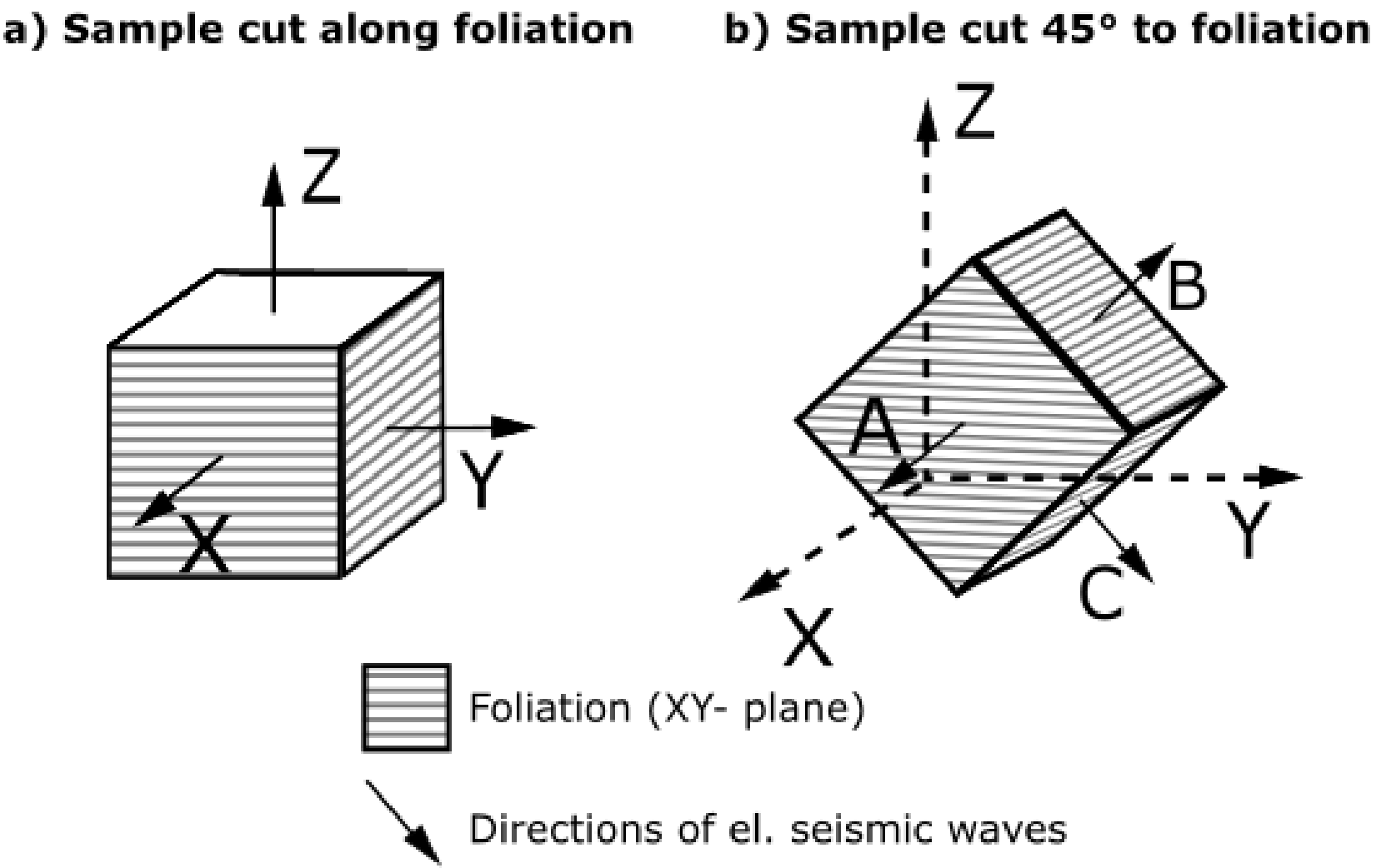

Control and Ram system

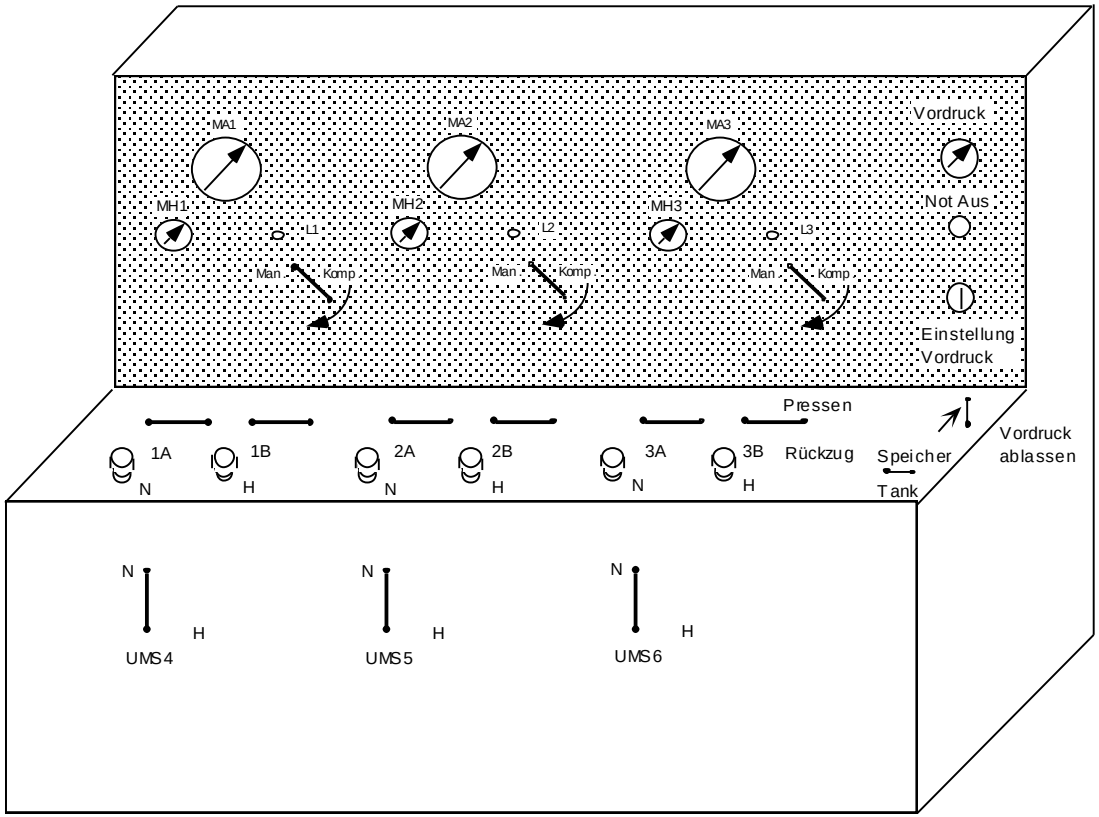

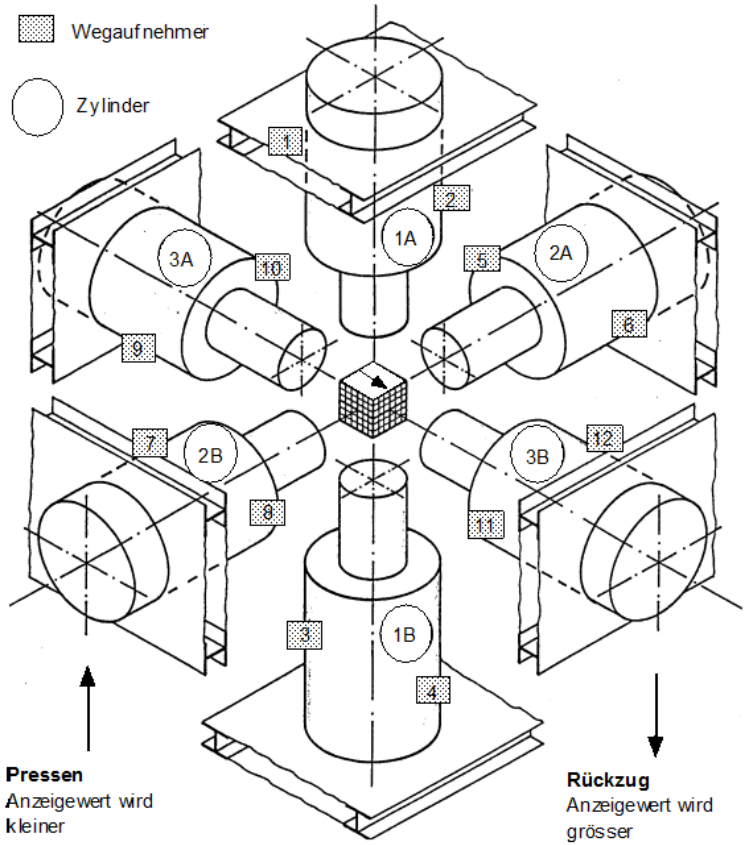

Loading control system

Loading ram system

Multi-anvil pressure apparatus

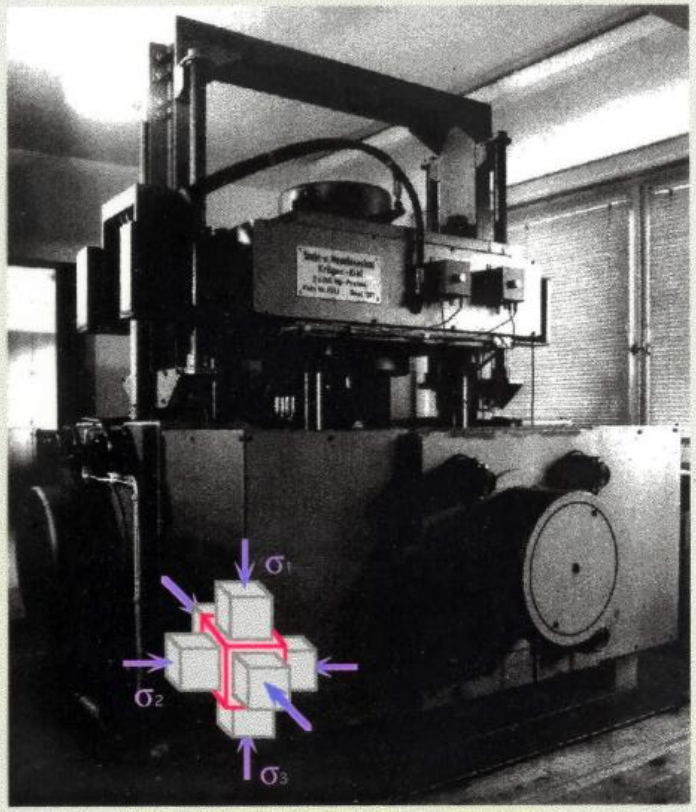

6 hydraulic rams (2000 kN)
edge length of the sample cube: 43 mm;
max. 750°C, 600 MPa (confining pressure)

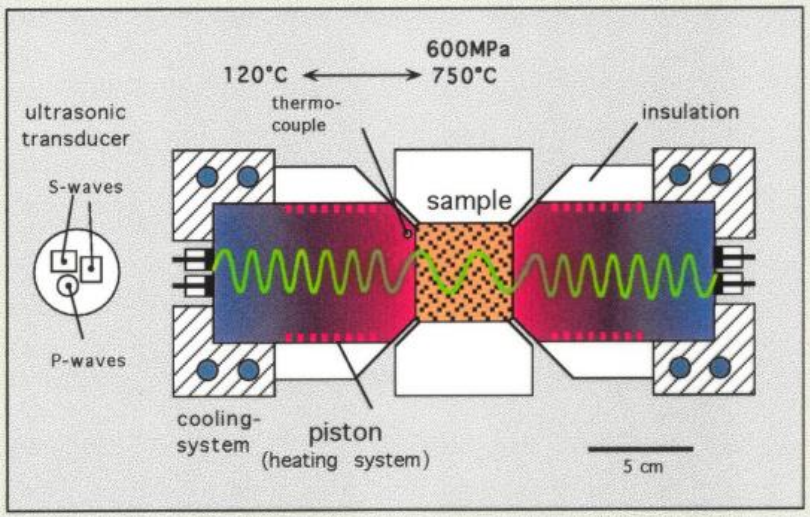

Piston - sample - transducer - assembly

Kern et al., (1997)

Process monitoring

- Effect of pressure and temperature on acoustic emissions

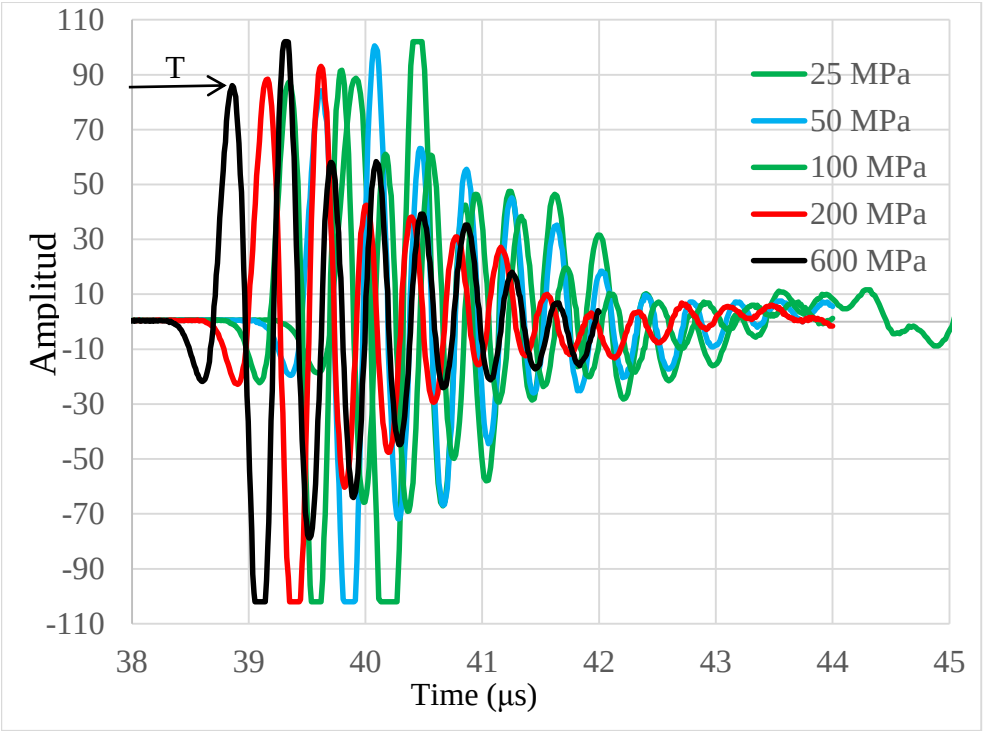

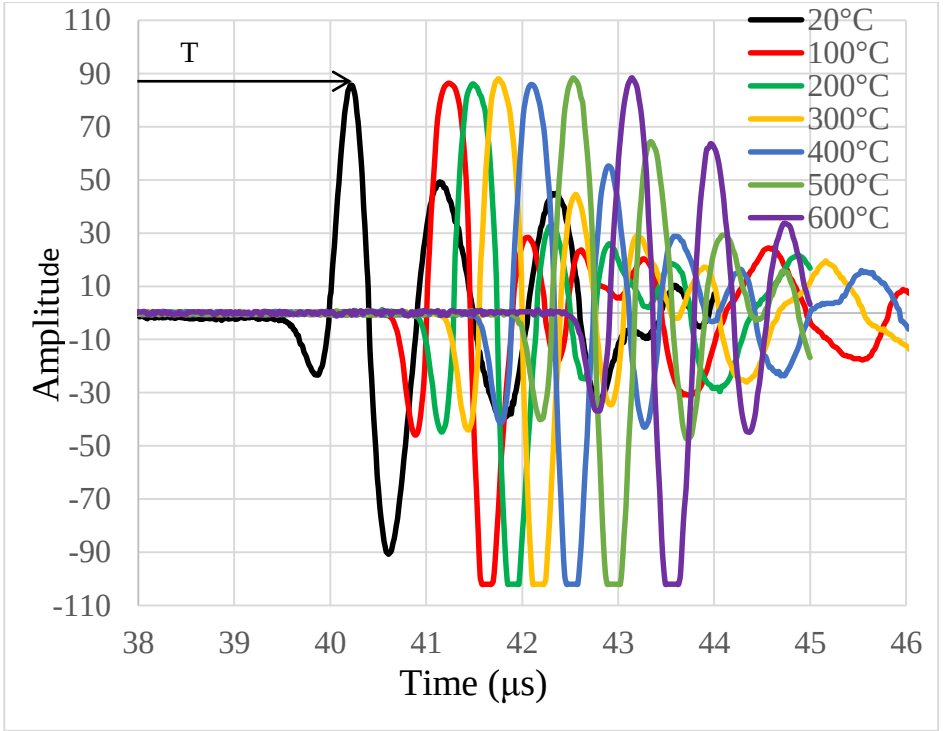

- Velocity calculation

$$Velocity = \frac{l_{cube}(\sigma, Temp.)}{T}; \; l_{cube} = \text{length of sample}$$

Effect of pressure and temperature

- Effect of pressure and temperature on seismic velocity
  $V_{in-situ} = V_0 + (dV/dP) * P_{in-situ} + (dV/dT)x * T_{in-situ}$

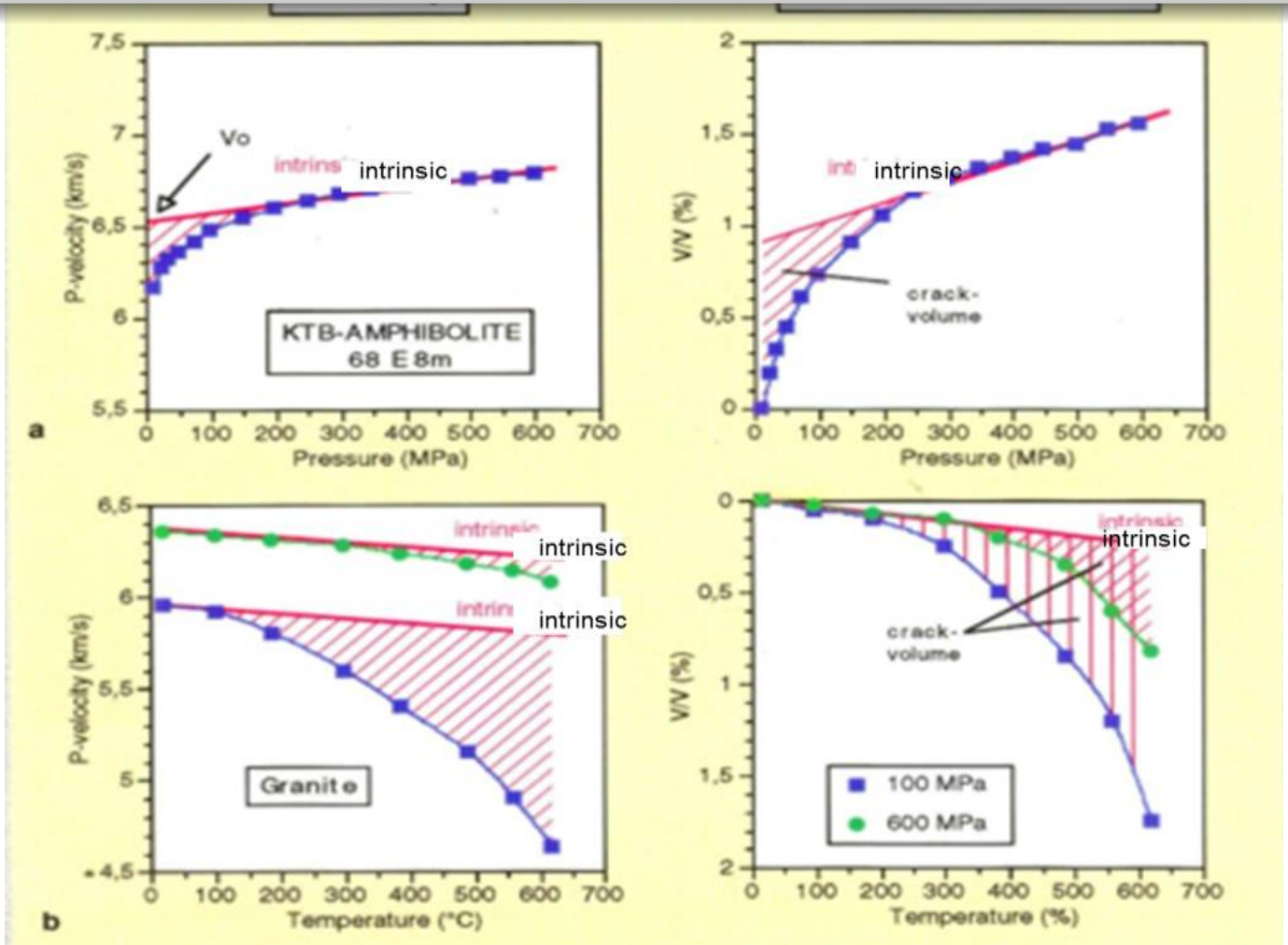

Velocity - density - chemistry (SiO_2) - relations

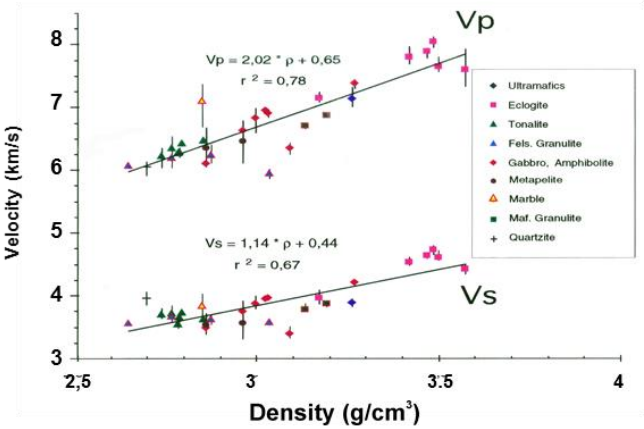

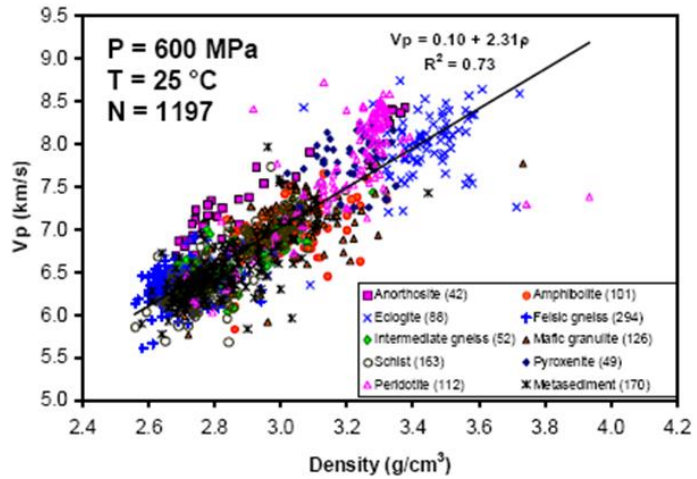

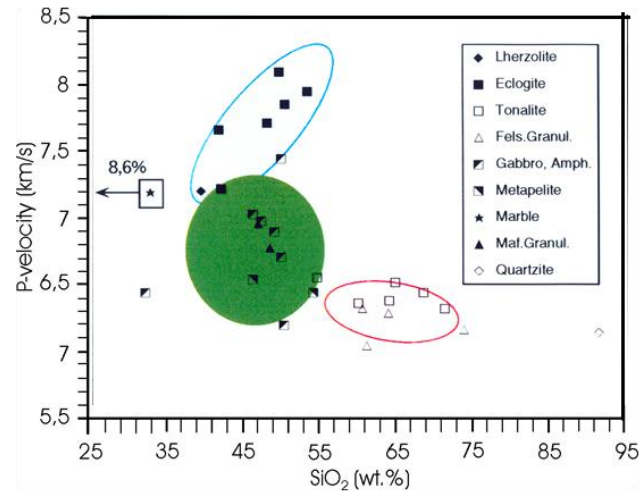

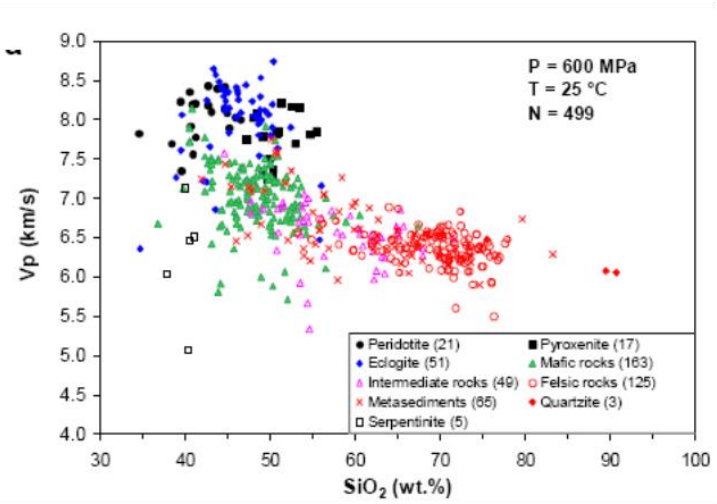

P-wave velocity versus density and SiO_2content of crustal rocks at 600 MPa and 25°C Left: UHP rocks-Dabie Mountains (after Kern et al, 1999) Right: Worldwide compilation (after Wang, 2004)

P-wave: Effect of pressure and temperature (rock sample)

- Directional dependence (anisotropy) of P-wave velocities with respect to the structural frame

Sample reference system

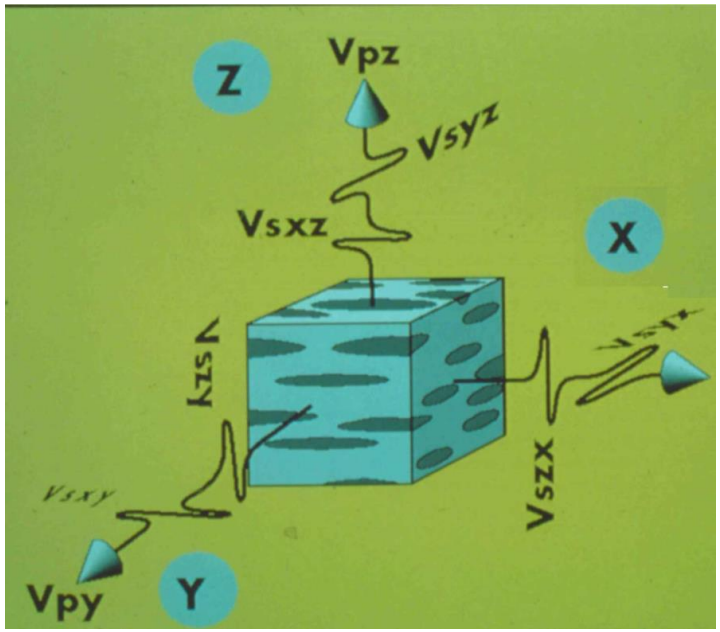

x = parallel to lineation and foliation,
y = normal to lination, parallel to foliation
z = normal to foliation

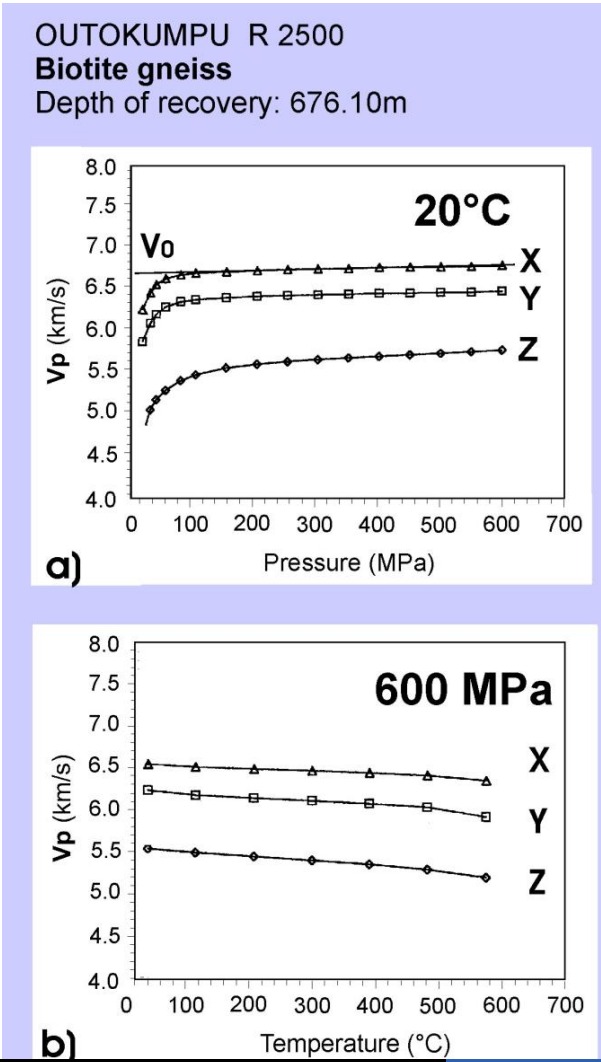

P and S -wave: Effect of pressure and temperature (steel sample)

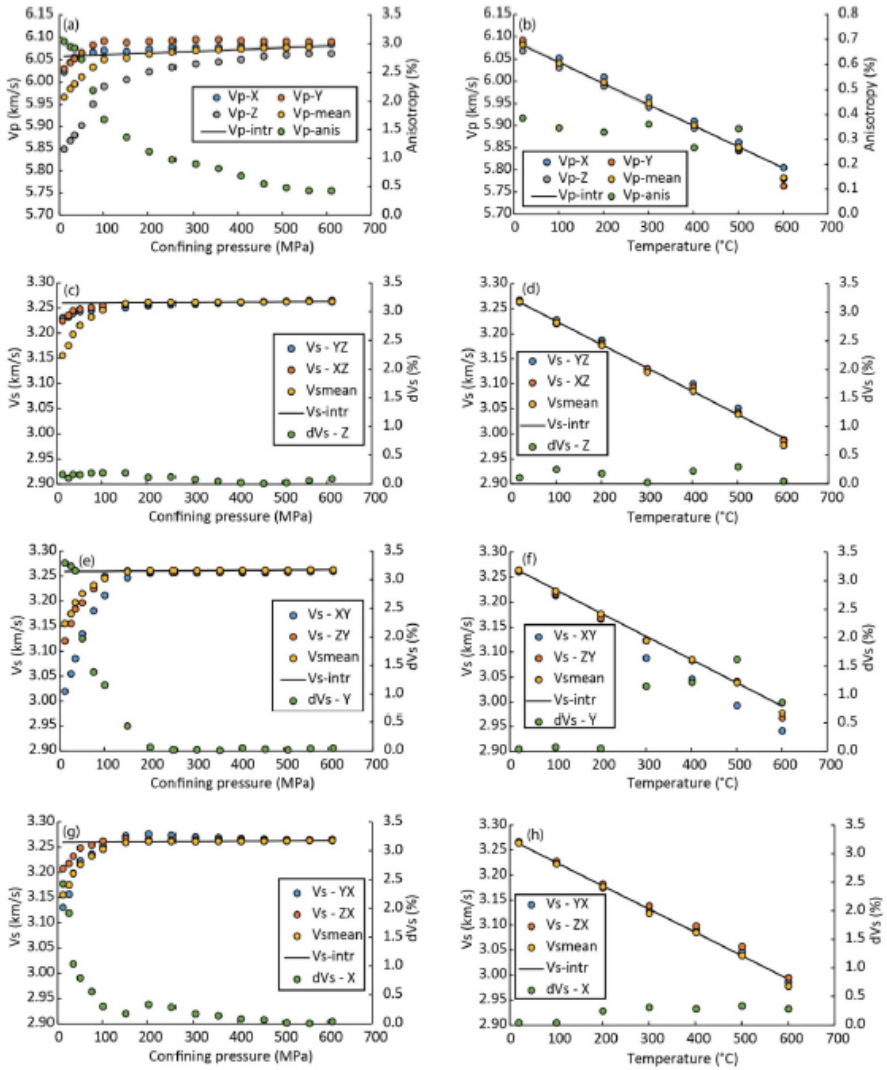

Bazargan et al., (2022)

Effect of forward and backward measurement

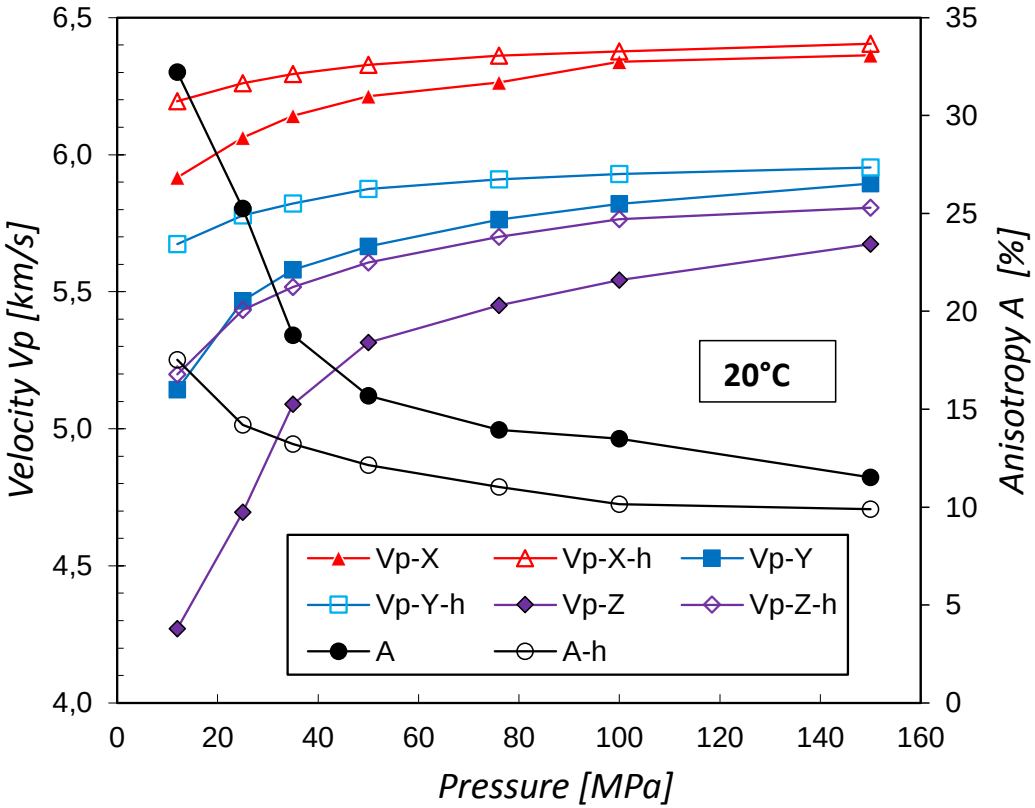

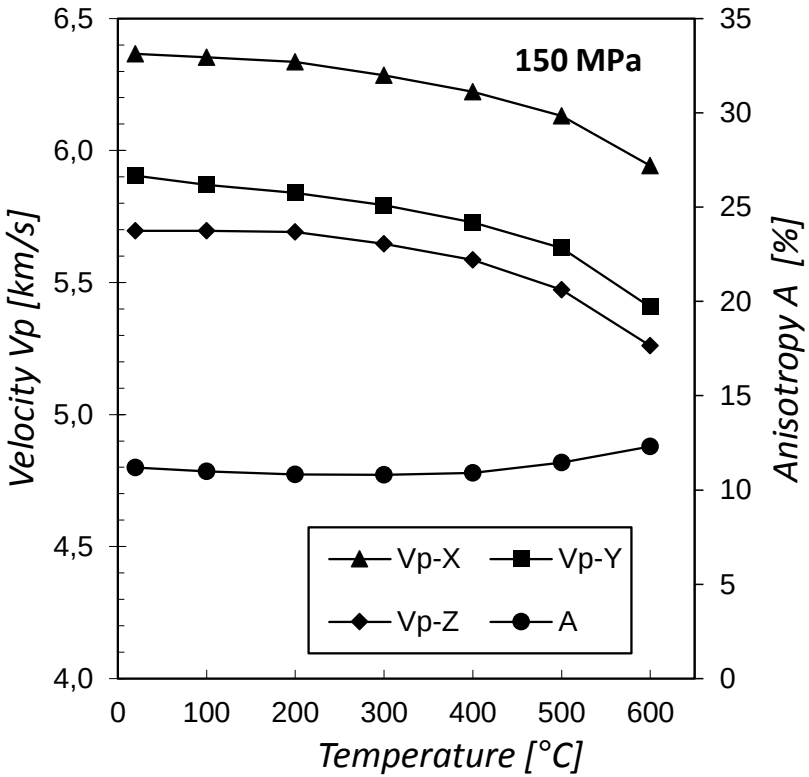

- Increase of confining pressure gives rise to a non-linear increase of P- and S-wave velocities due to progressive closure of microcracks.
- The opening of new cracks or widening of existing cracks causes decreasing P-and S-wave velocities.

Pressure and temperature effect on microcracks

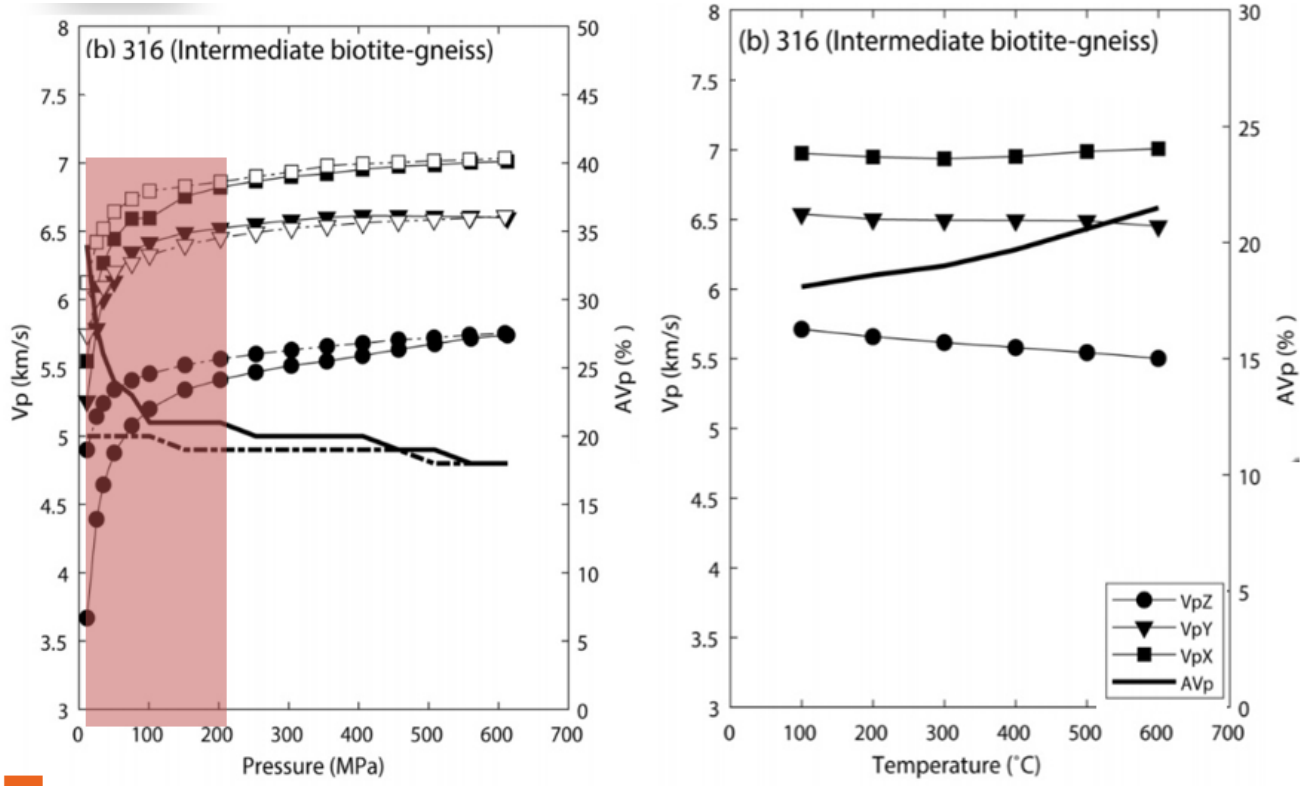

Bazargan et al., (2022)

- Increase of confining pressure gives rise to a non-linear increase of P- and S-wave velocities due to progressive closure of microcracks.
- The opening of new cracks or widening of existing cracks causes decreasing P-and S-wave velocities.

Anisotropy

Causes of anisotropy of physical properties in geomaterials

- Crystallographic preferred orientation (CPO)
- Preferred morphological or shape preferred orientation (SPO)
- Preferred orientation of (fluid-filled) microcracks
- Thin layers of isotropic material with different properties

Sample result of anisotropy

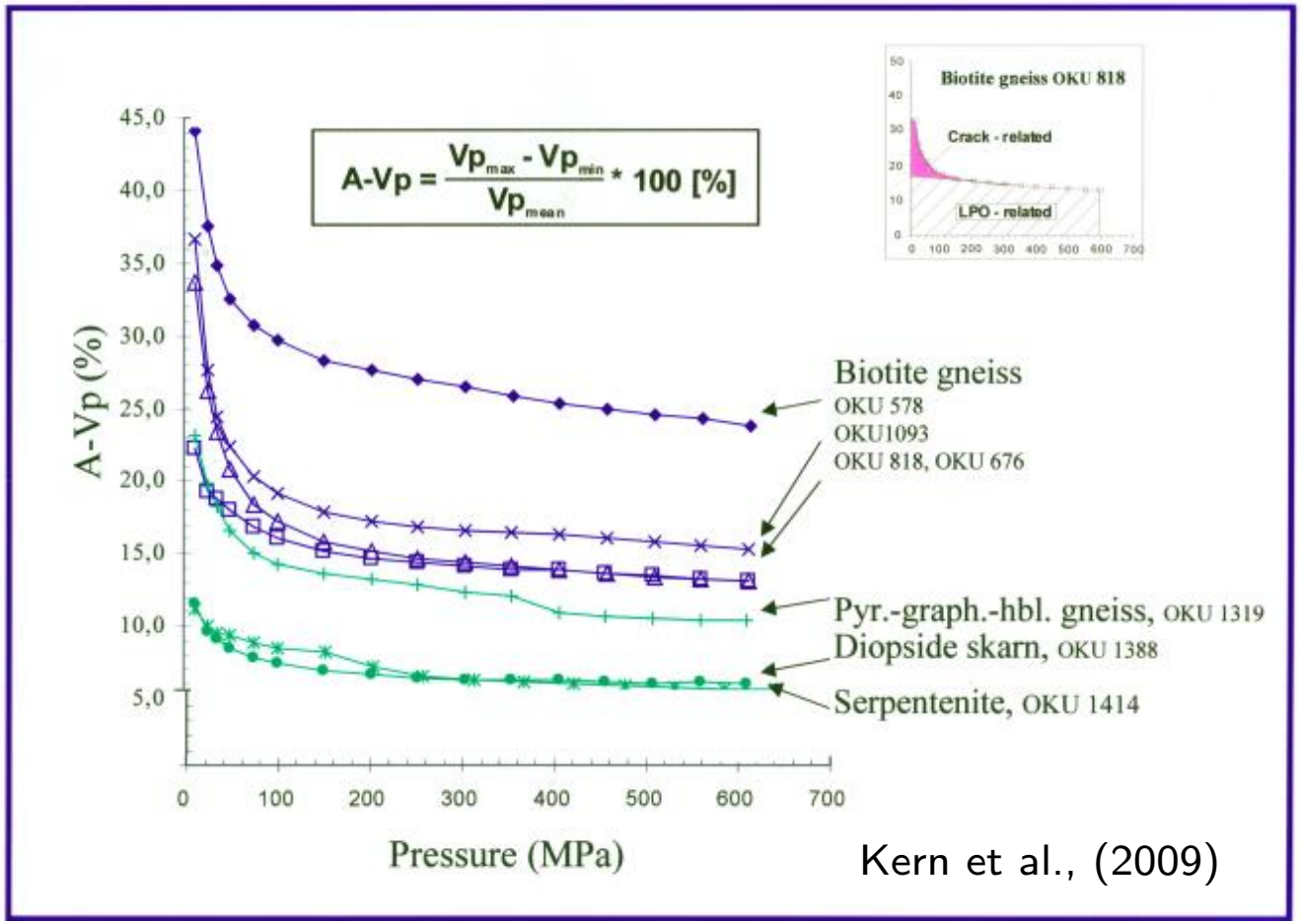

Kern et al., (2009)

- Anisotropy of P-wave velocities and contribution of oriented cracks and crystallographic preferred orientation (CPO) to bulk anisotropy at different pressures

Ranges of Vp-anisotropy

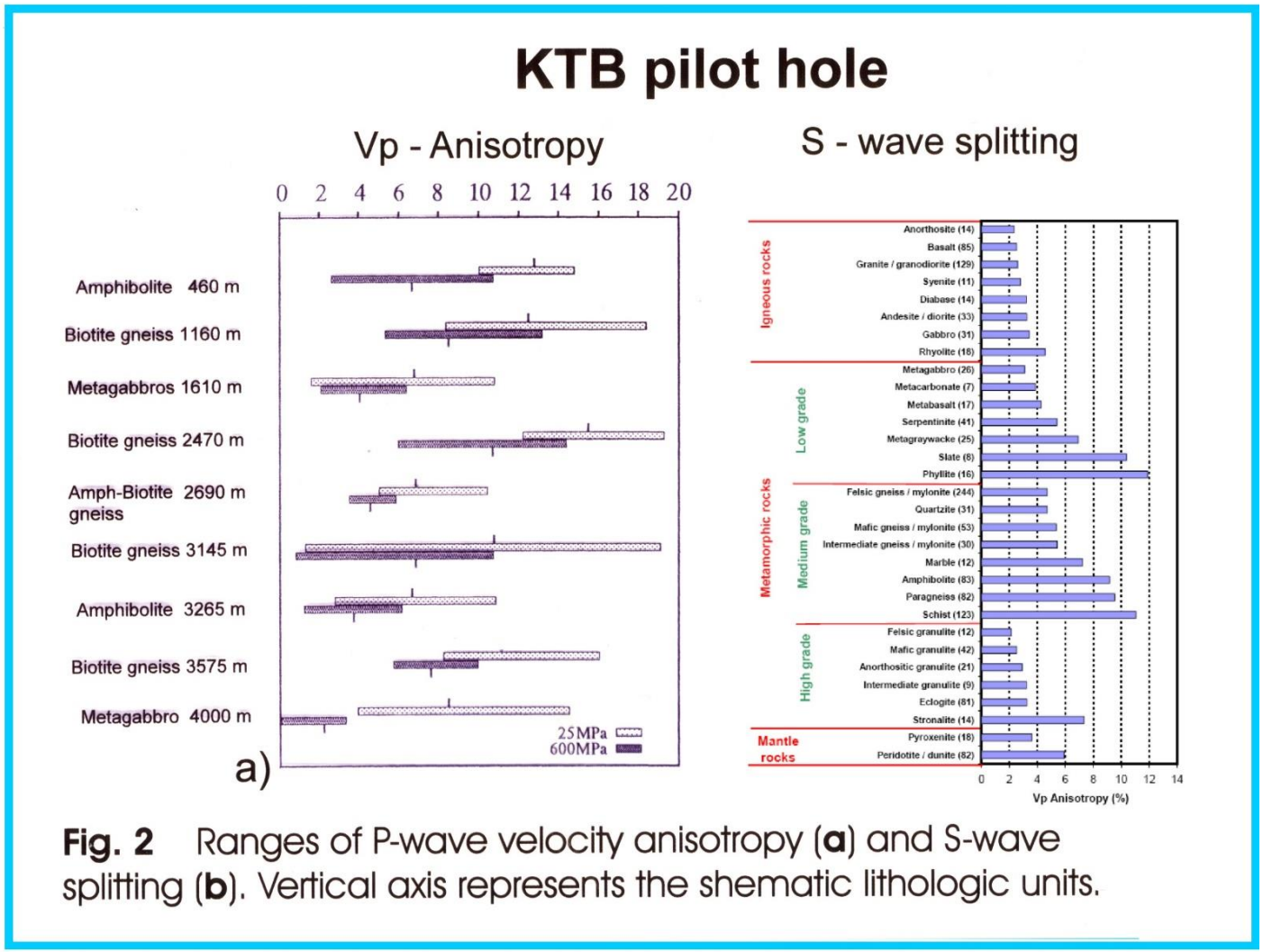

Fig. 2 Ranges of P-wave velocity anisotropy (**a**) and S-wave splitting (**b**). Vertical axis represents the shematic lithologic units.

Ranges of Vp-anisotropy (Kern et al, 1991)

Vp-anisotropy in crustal and mantle rocks at 600 MPa (compiled by Wang, 2004)

S-wave-splitting

Shear-wave-splitting

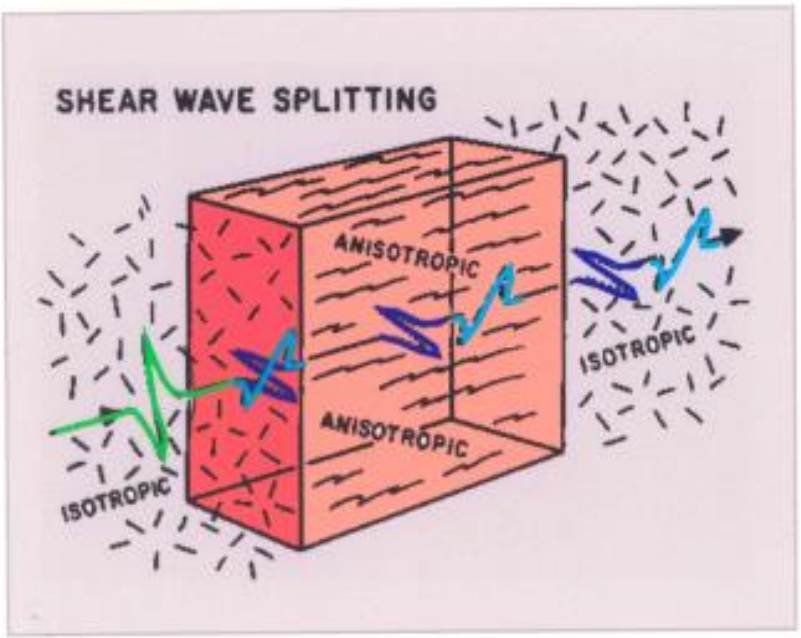

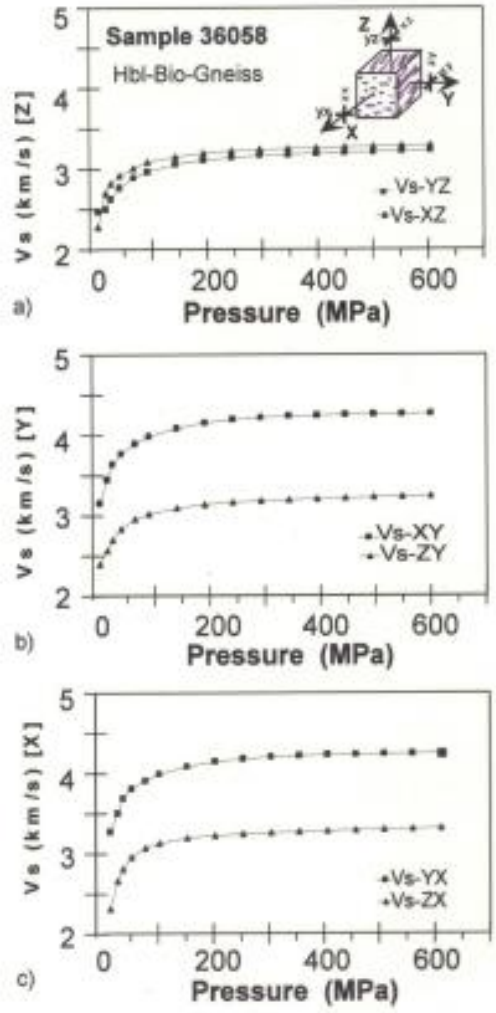

S-wave-splitting:forward and backward

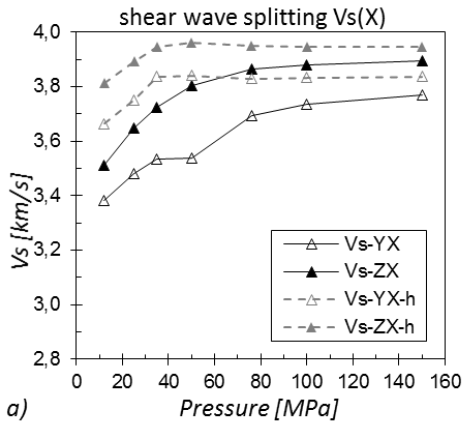

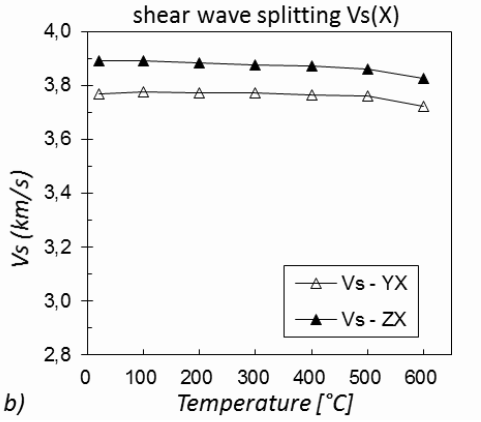

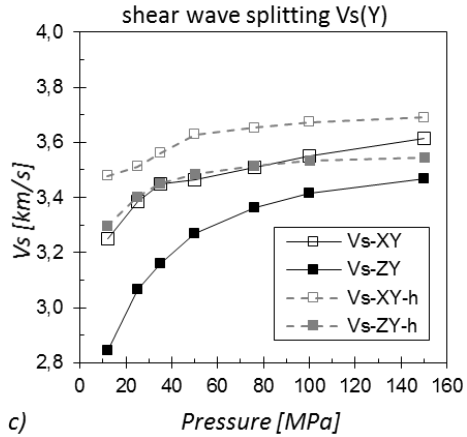

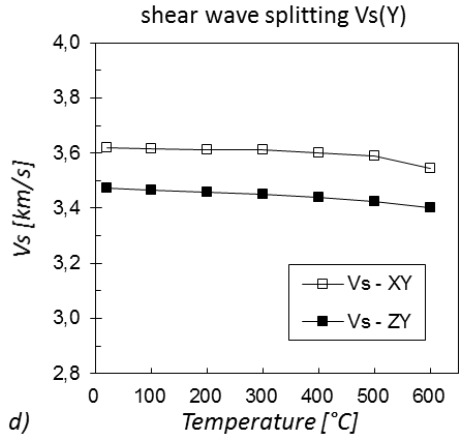

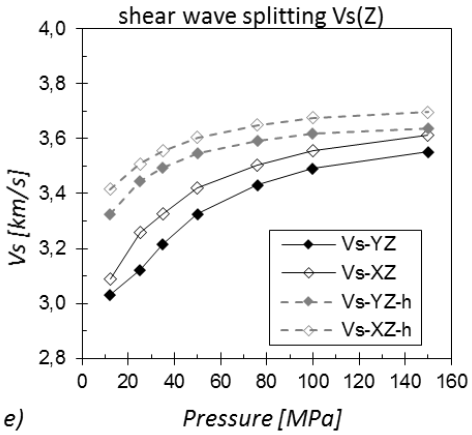

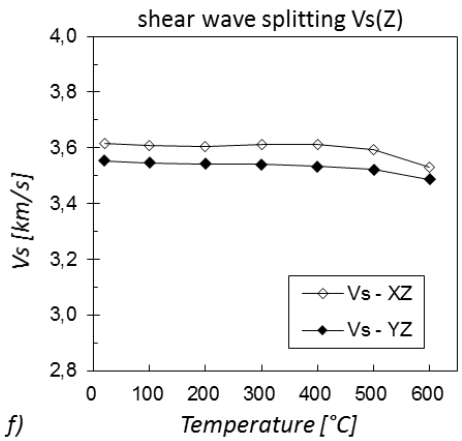

- Backward P-and S-wave velocity are larger than forward measurement, due to closure of existing (open) cracks

Poisson's ratio

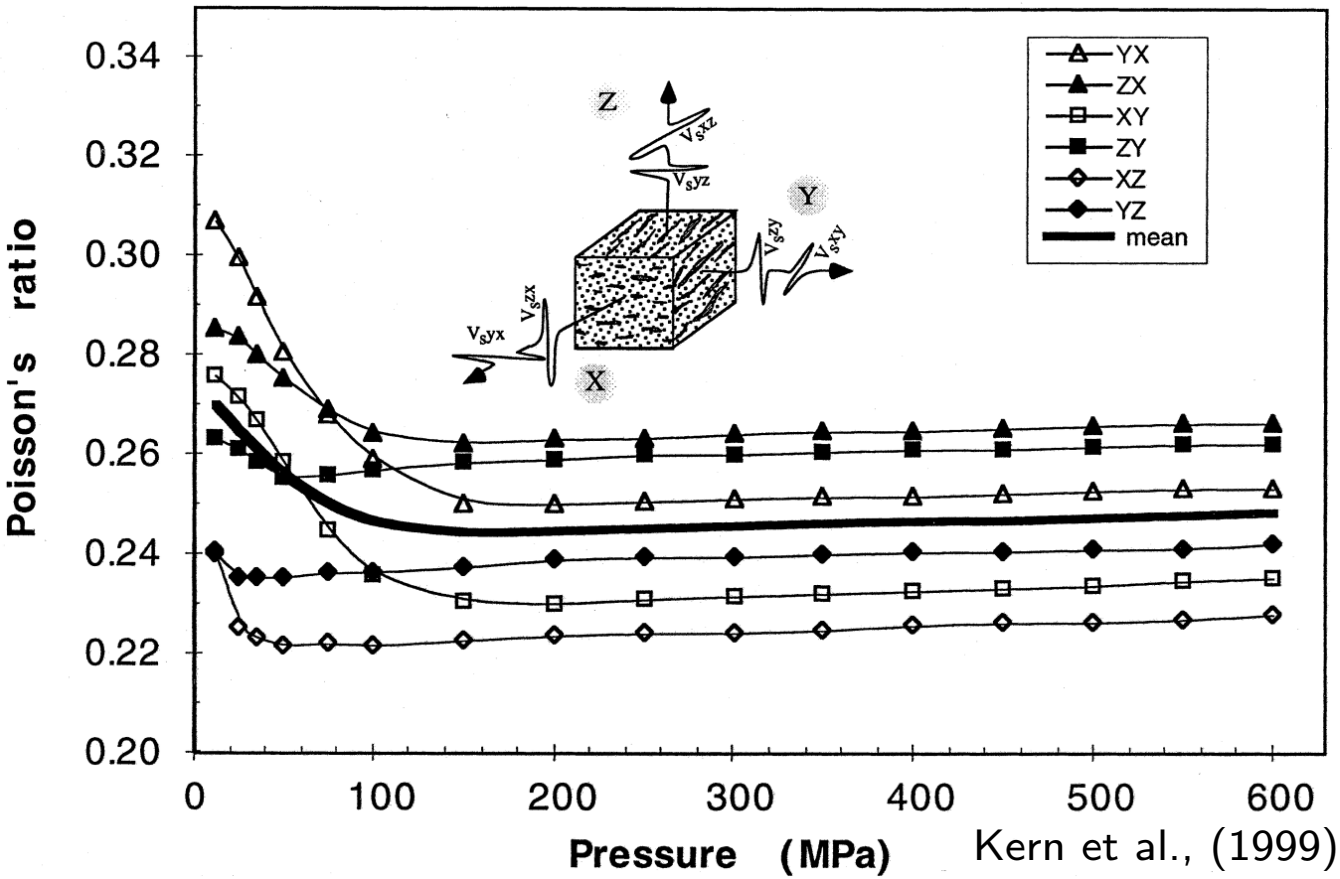

Kern et al., (1999)

Average Poisson ratio and the variation of the Poisson's ratio with pressure regarding to direction of wave propagation and shear wave polarization.

Volumetric strain and density

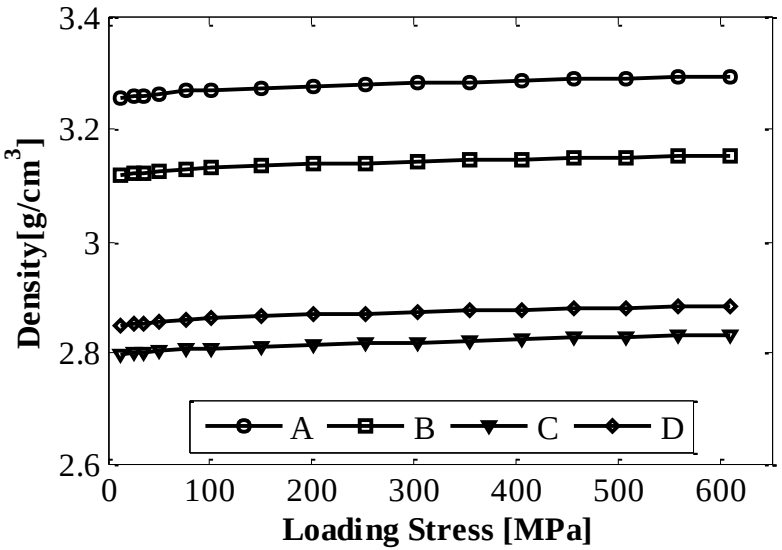

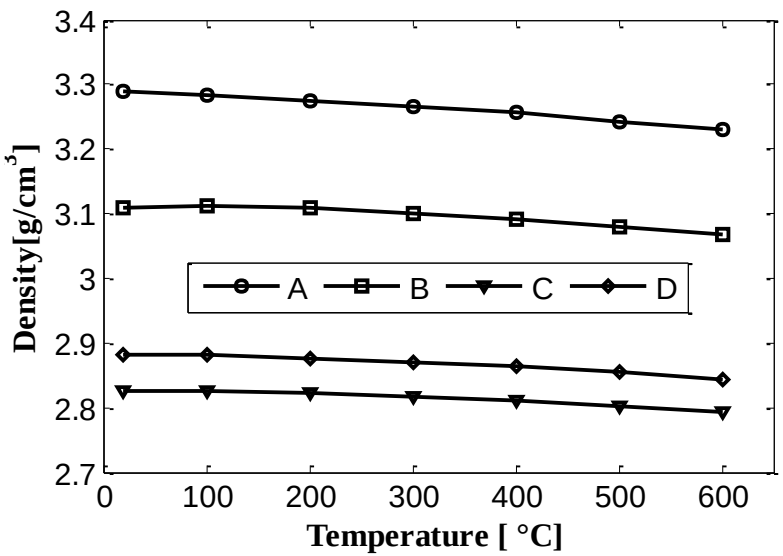

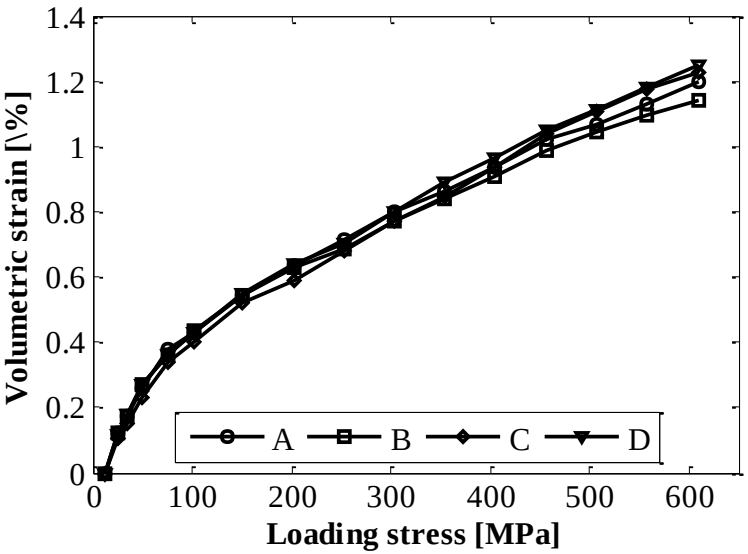

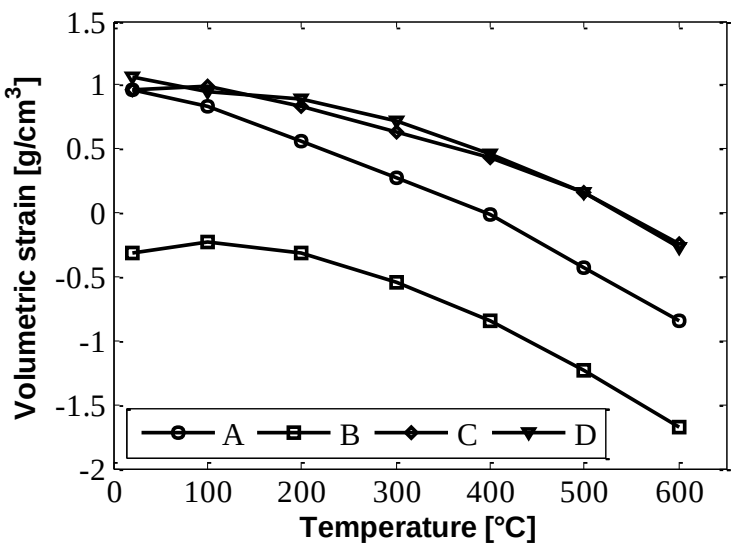

Elastic Constants: rock sample

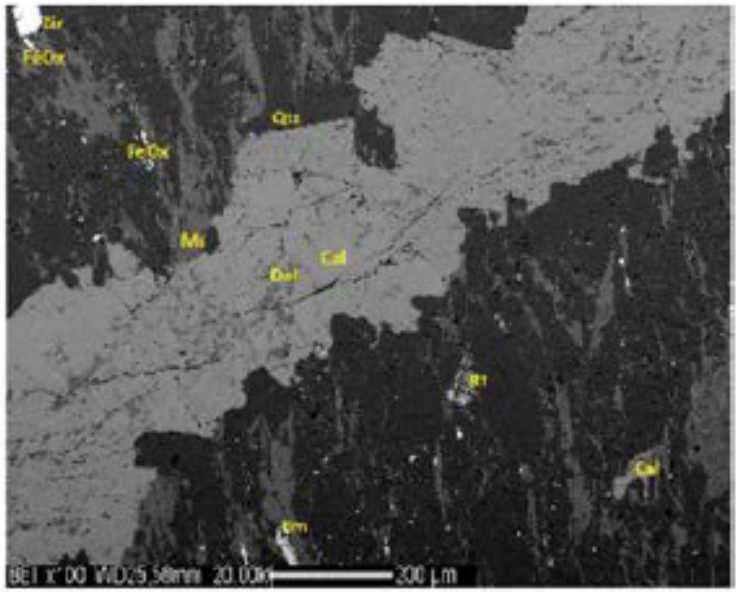

Sample depth: 3289.6-3296.2m, composed of hornblende, biotite, quartz, minor apatite, titanite and features a density of 2.936 g/cm^3, planar schistosity and strong foliation, relatively small grain sizes

Motra et al., (2018)

Elastic Constants: V_p and anisotropy as a function of pressure and temperature

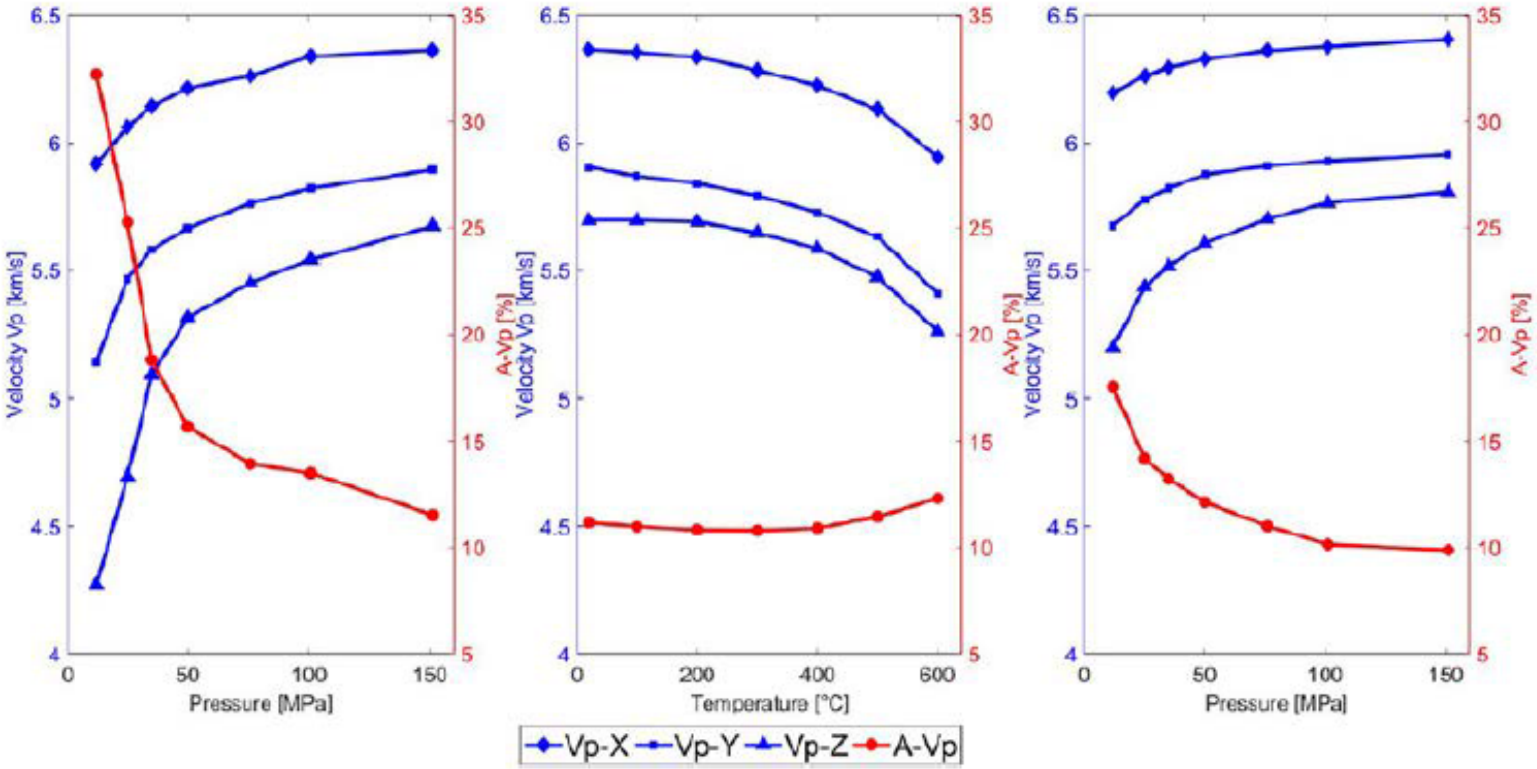

V_P wave velocities and V_p wave anisotropy an a function of loading, temperature and unloading

Motra et al., (2018)

Elastic Constants (VTI Symmetry)

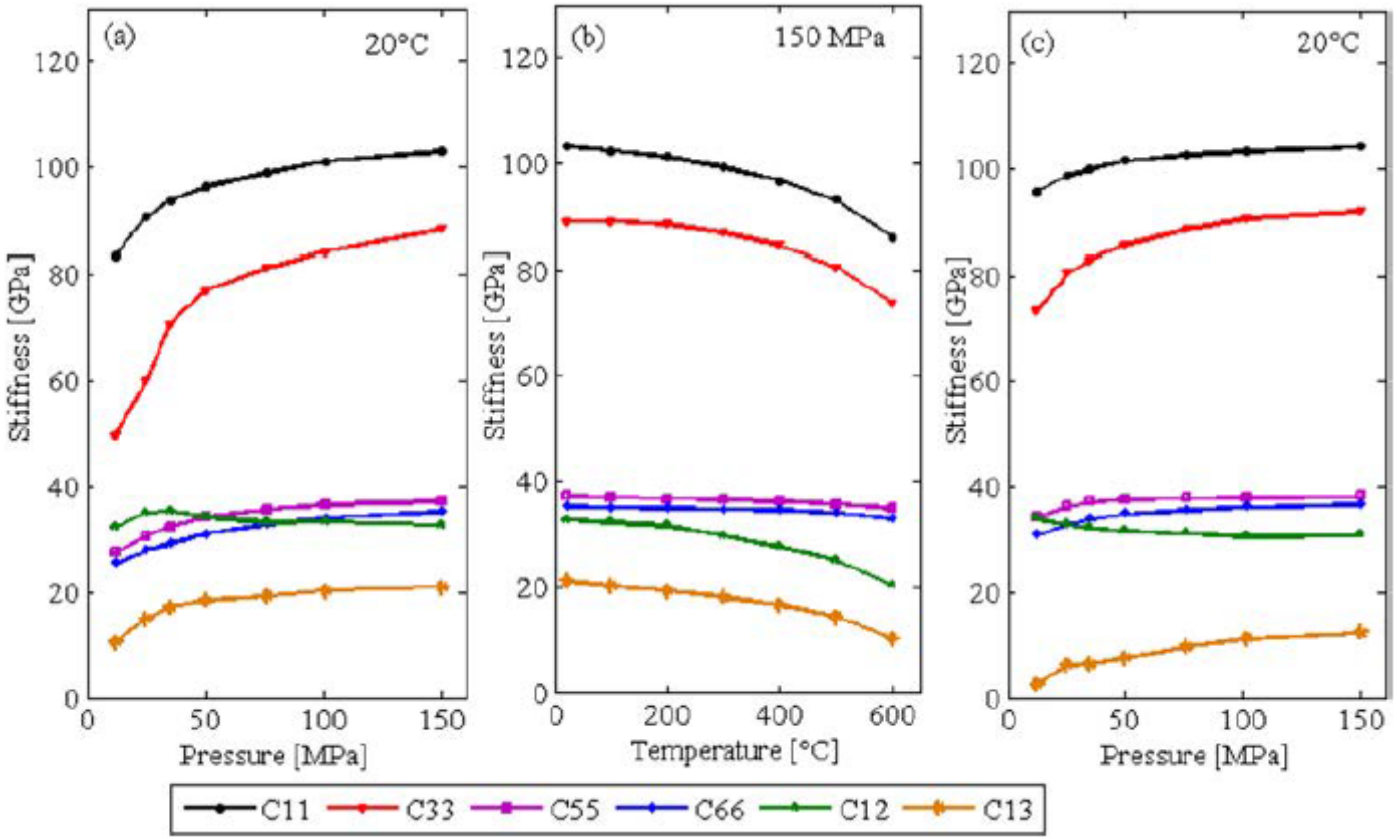

Elastic Constants (VTI Symmetry, (a) as a function of pressure at constant room temperature (b) as a function of temperature at constant pressure 150 MPa (c) unloading at constant room temperature) (figure a and c look similar, mention "loading" on figure a and "unloading" on figure c)

Motra et al., (2018)

Elastic Constants (Orthorhombic Symmetry)

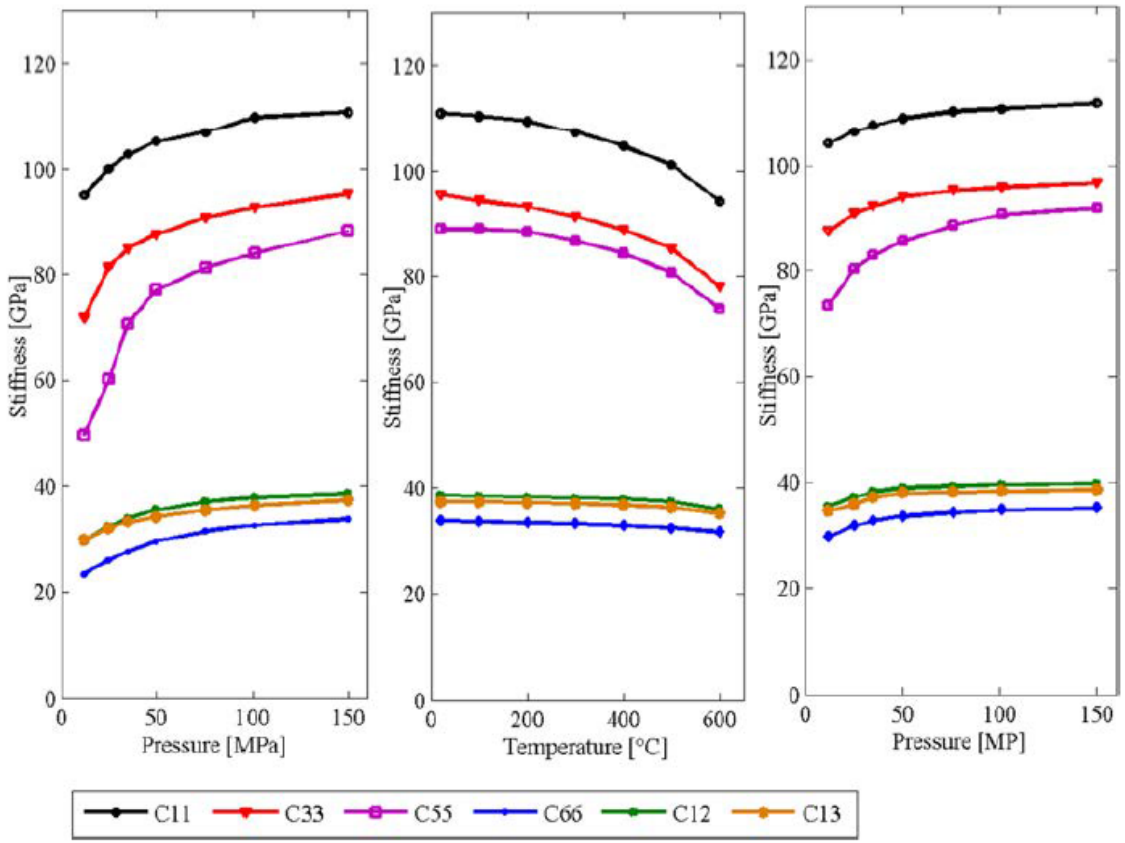

Elastic Constants (Orthorhombic Symmetry, (a) as a function of pressure at constant room temperature (b) as a function of temperature at constant pressure 150 MPa (c) Unloading at constant room temperature)(mention "loaded" on figure a and "unloaded" on the figure c)

Motra et al., (2018)

Influence of grain size (Gabbro)

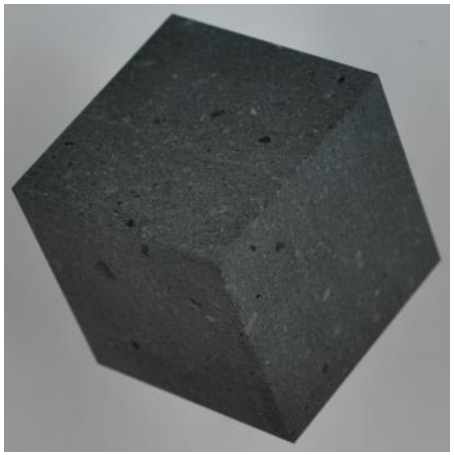

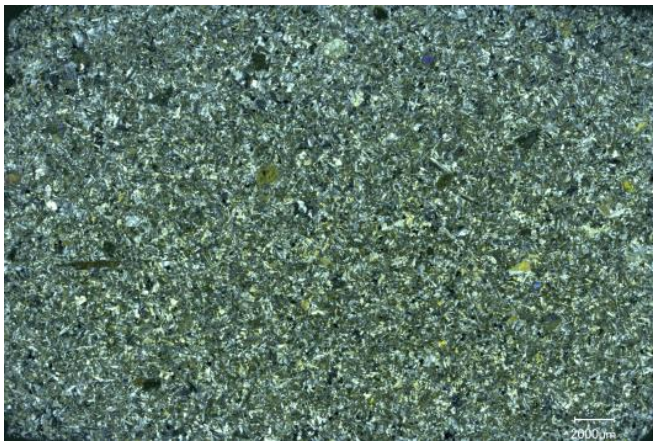

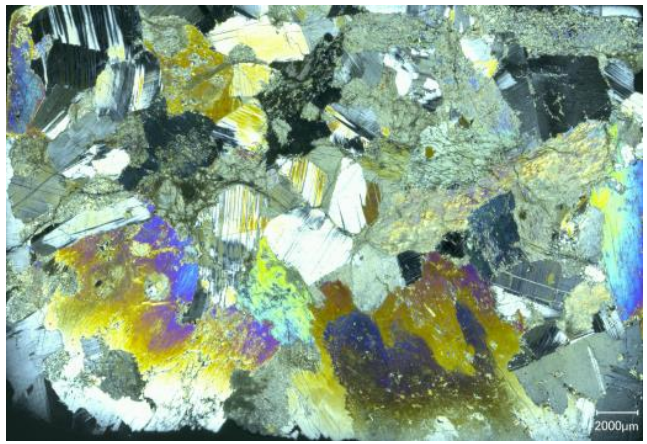

Fine grain (0.19 - 0.4 mm), medium grain (1.7 - 2.0 mm), coarse grain (3.8 - 5.3 mm)

Influence of grain size (Gabbro)

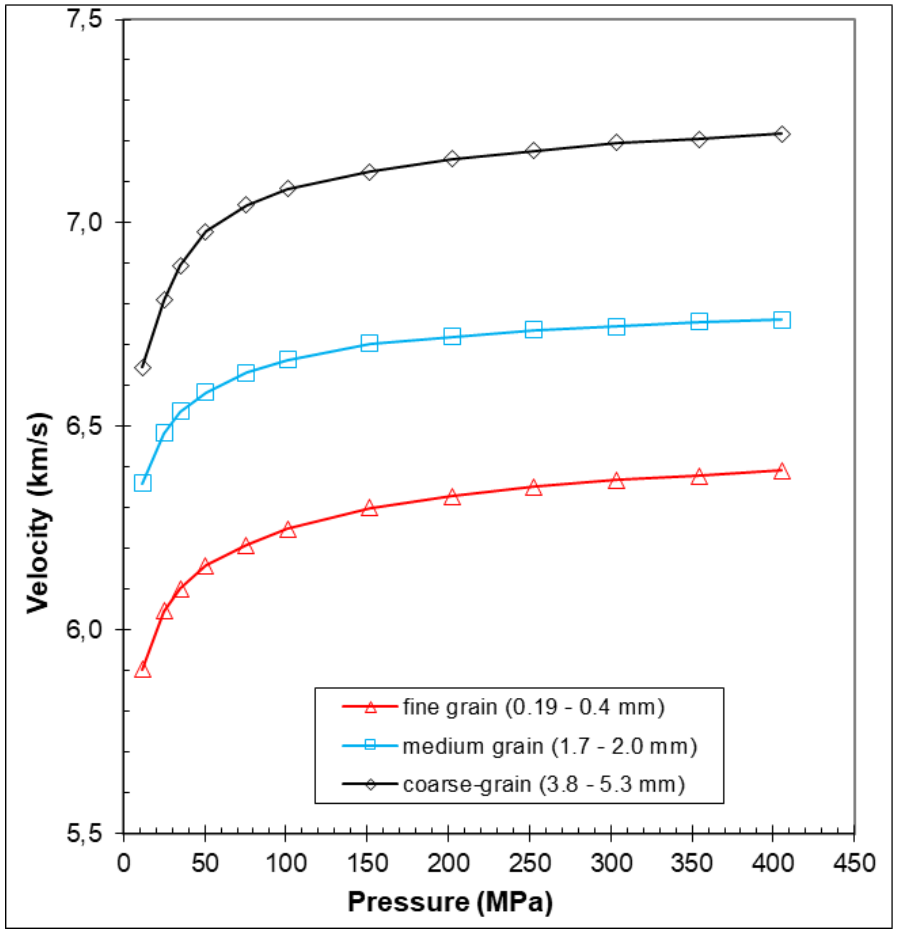

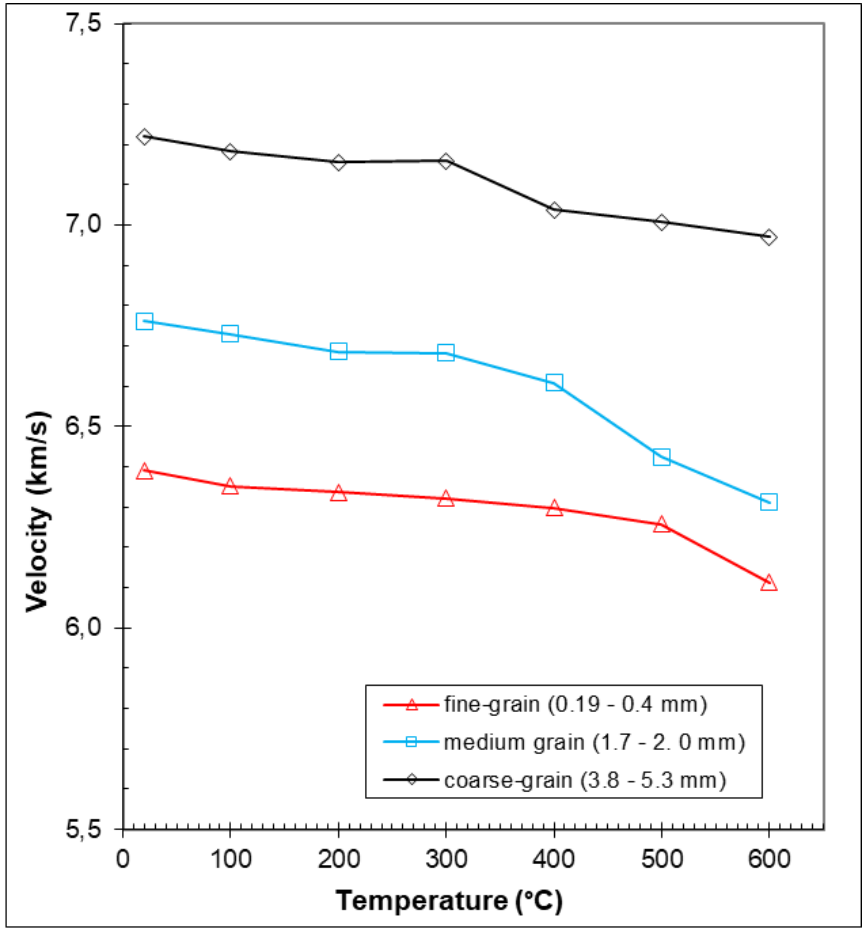

- Porosity decrease as the grain size increases
- Decrease in mechanical properties with decreasing grain size of the materials
- Grain will influence: porosity, permeability, mineralogy and specific surface area

Seismic properties – porosity vs. grain size?

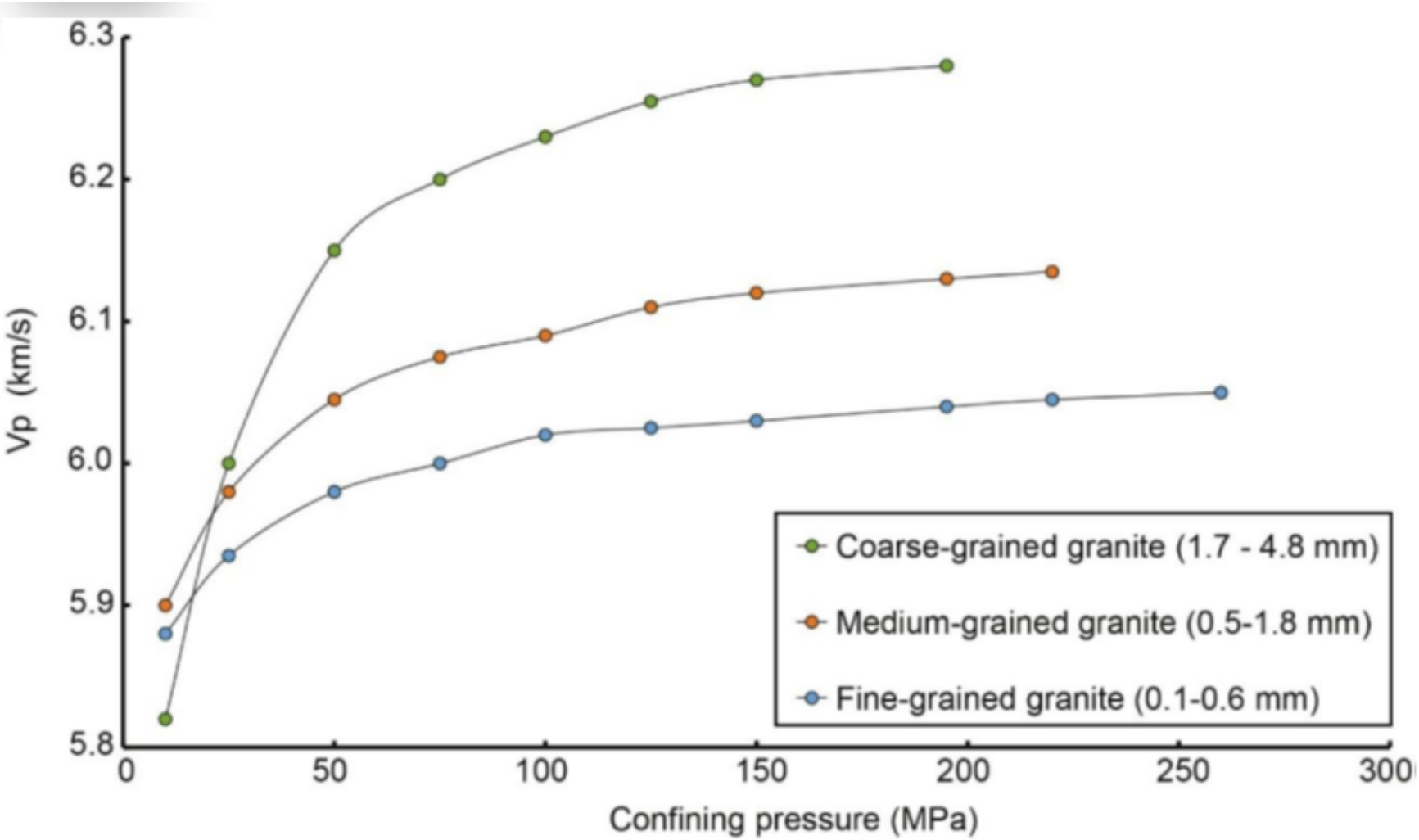

Lebedev et al., 1974

Calculation of the 3D velocity distribution

Part II

1. Use of Elastic stiffness coefficients C_{ijkl} of the constituent minerals (from literature)
2. Determination of model composition
   1. Standard point counting
   2. Microscopic image analysis
   3. Mass balance calculation from chemical composition of bulk rock and its constituent minerals (large volume)
3. Measurement of crystallographic preferred orientation (CPO)
   1. U-stage
   2. X-ray or neutron texture goniometry
   3. SEM equipped with an electron backscatter diffraction (EBSD) system

3D velocity calculation

- Calculation of the whole-rock (aggregate) velocities

$$V(rock) = \sum_{i=1}^{n} X_i V_i$$

where n is the number of minerals in the aggregate, X_i the volume fraction of each mineral, and V_i the isotropic aggregate velocity of each mineral (VRH average)

- **Model composition**: Mass balance calculation from chemical composition of bulk rock (XRF) and the constituent minerals (microprobe)
- **Isotropic aggregate velocities**: VRH averages; Literature data (Gebrande, 1982)

3D velocity calculation

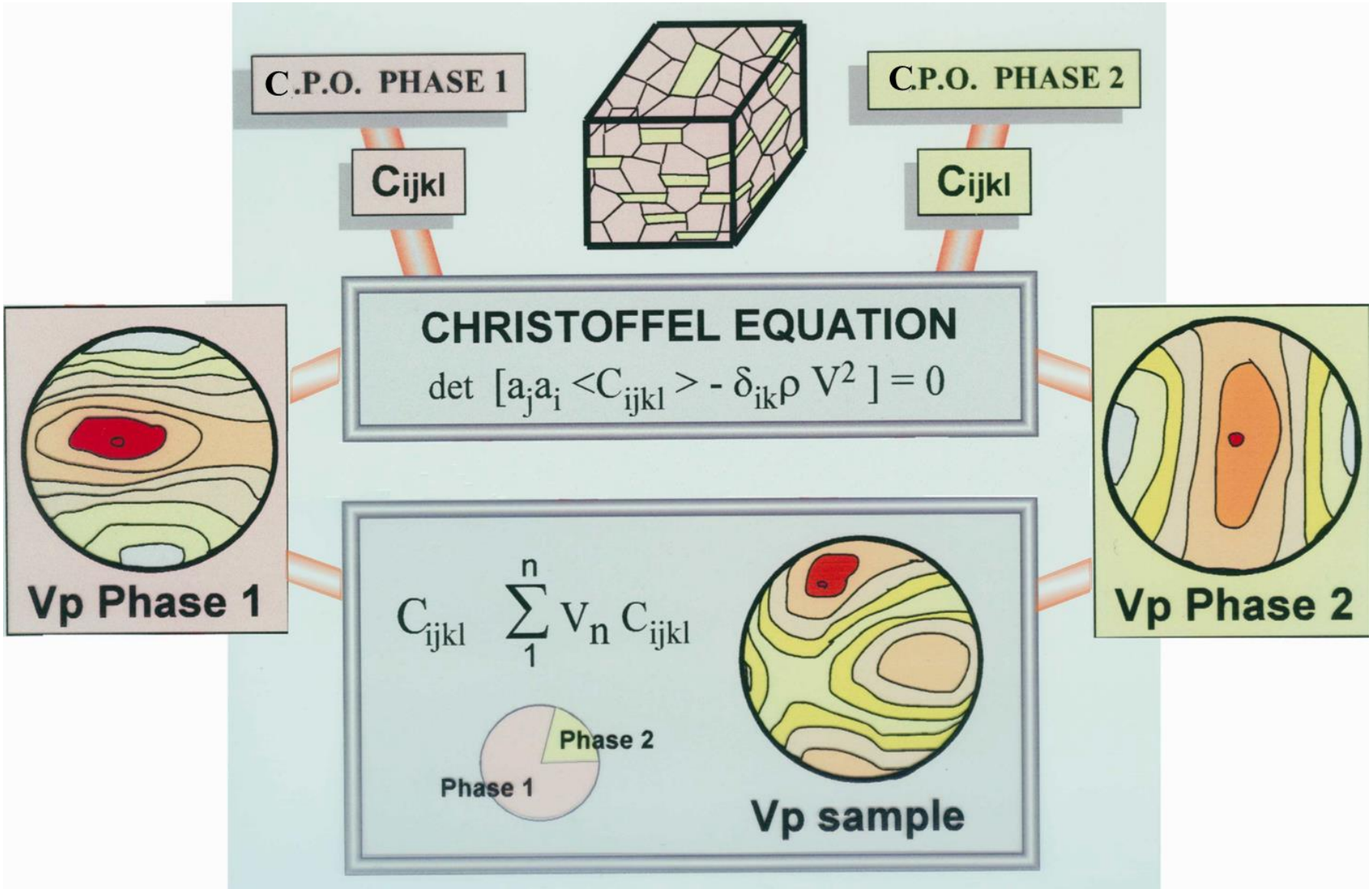

3D elastic velocities from elasticity stiffness

Vp (km/s)

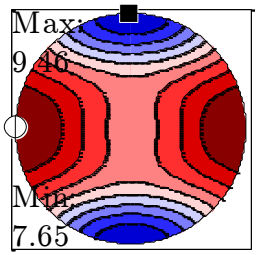

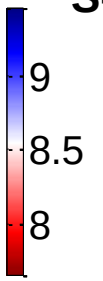

S-wave anisotropy (%)

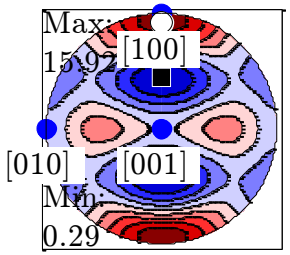

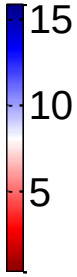

Vs1 polarization

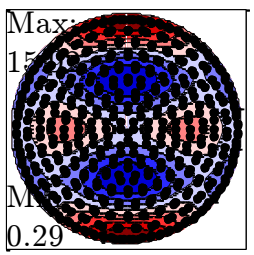

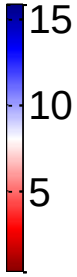

Vp Anisotropy = 21.2 **Max Vs Anisotropy = 15.9**

Vs1 (km/s)

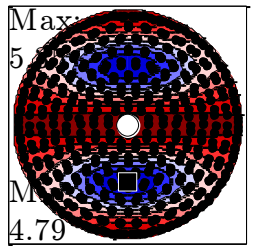

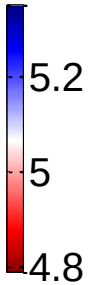

Vs2 (km/s)

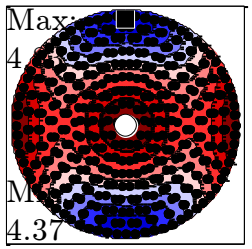

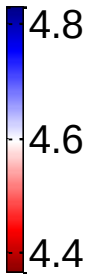

dVs=Vs1-Vs2 (km/s)

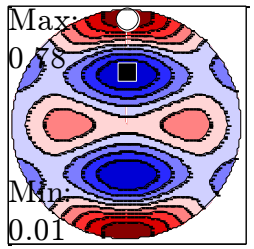

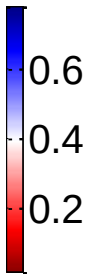

Vs1 Anisotropy = 11.0 **Vs2 Anisotropy = 10.1** **Max dVs (km/s) = 0.79**

Vp/Vs1

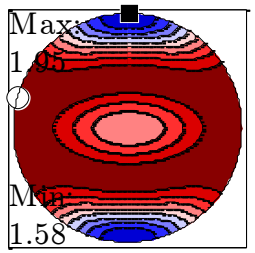

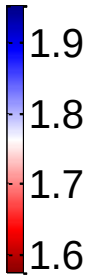

Vp/Vs2

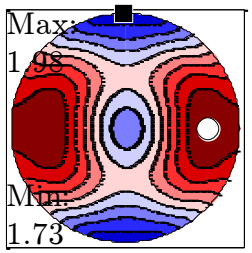

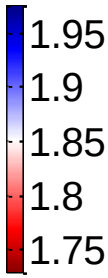

Vp/Vs1 Anisotropy = 21.4 **Vp/Vs2 Anisotropy = 13.3**

Microscopic observation of micro-structurs

Observation: before test

- Microscopic observation of microstructures of minerals
- Minerals and chemical composition
- Microcracks

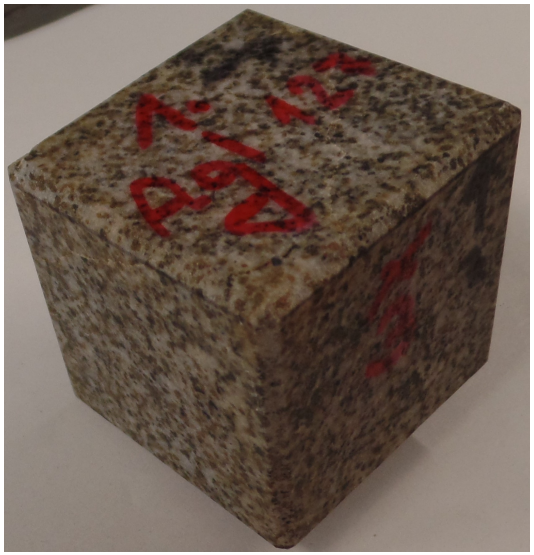

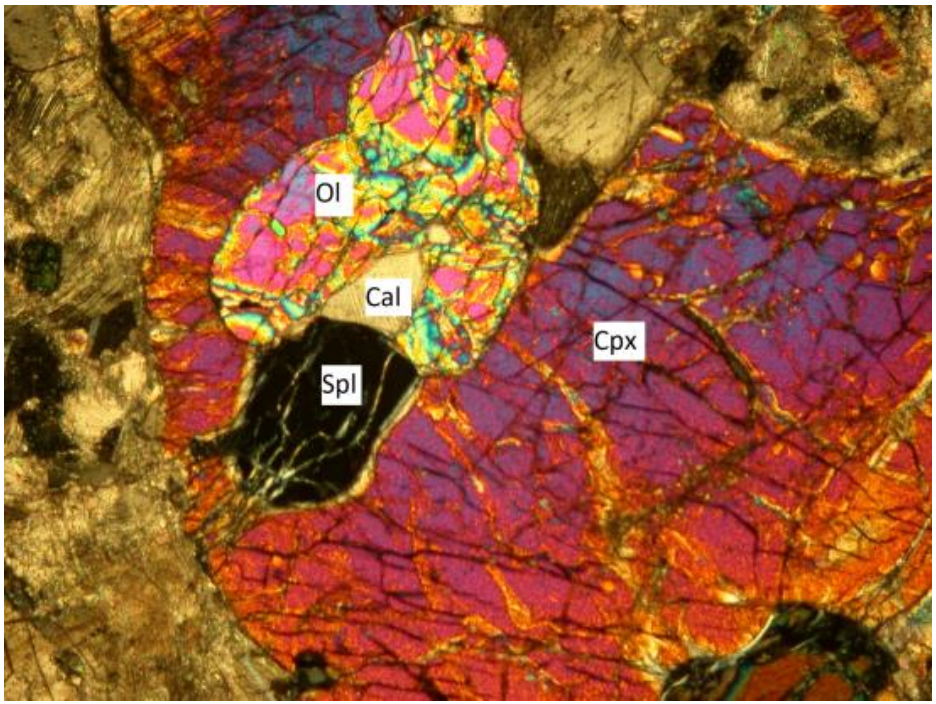

Sedimentary rock: Minerals

- 65% Calcite, 20% Olivin, 5% Spine, 5% Dolomite, 5% Clinopyoxen, Serpentine, Mineral ores
- Density: 2.86 g/cm^3

Thermodynamic modelling

- P-T condition is realized with the free Gibbs energy minimization [Connolly and Kerrich, 2002; Connolly, 2009] algorithm
- Calculating seismic wave velocities at any pressure and temperature using classical thermodynamics equations, databases, solution models, and knowing the bulk composition of the system (The Perple-X software package)

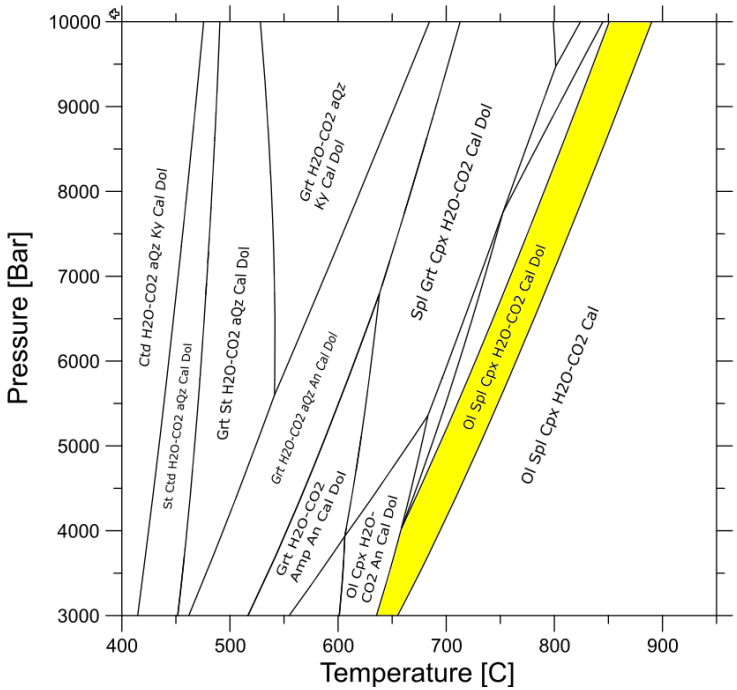

- Mean velocity from measurement: 6.50 km/s (Vp); mean velocity from measurement: 3.40 km/s (Vs)
- Mean velocity from modeling: 7,60 km/s (Vp); mean velocity modeling: 4.10 km/s (Vs)

Mantel rock: granulite and ecogite

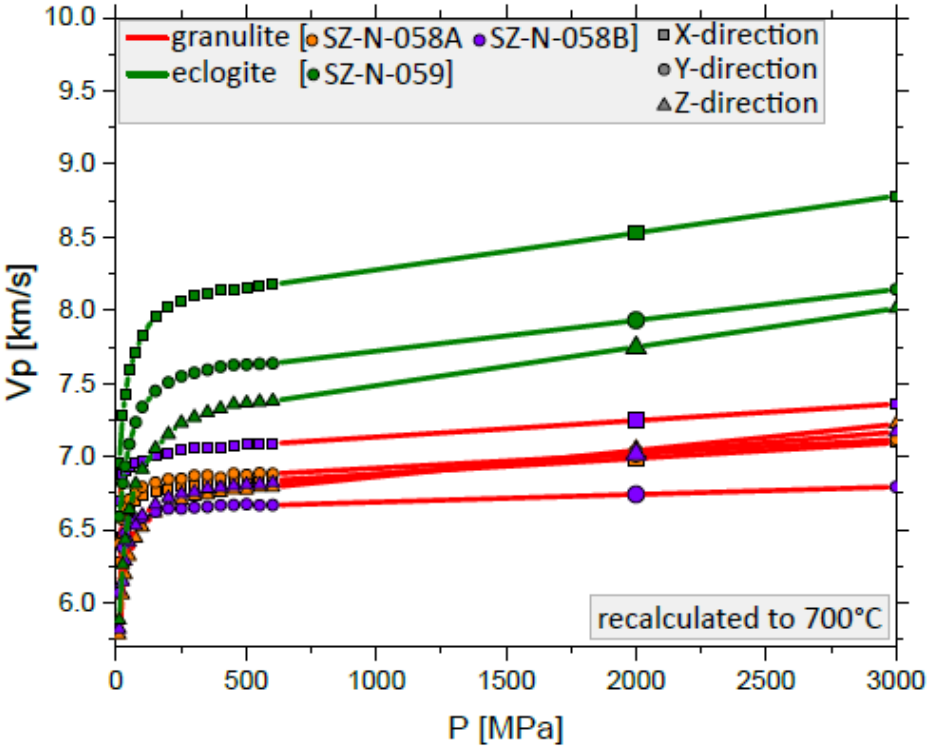

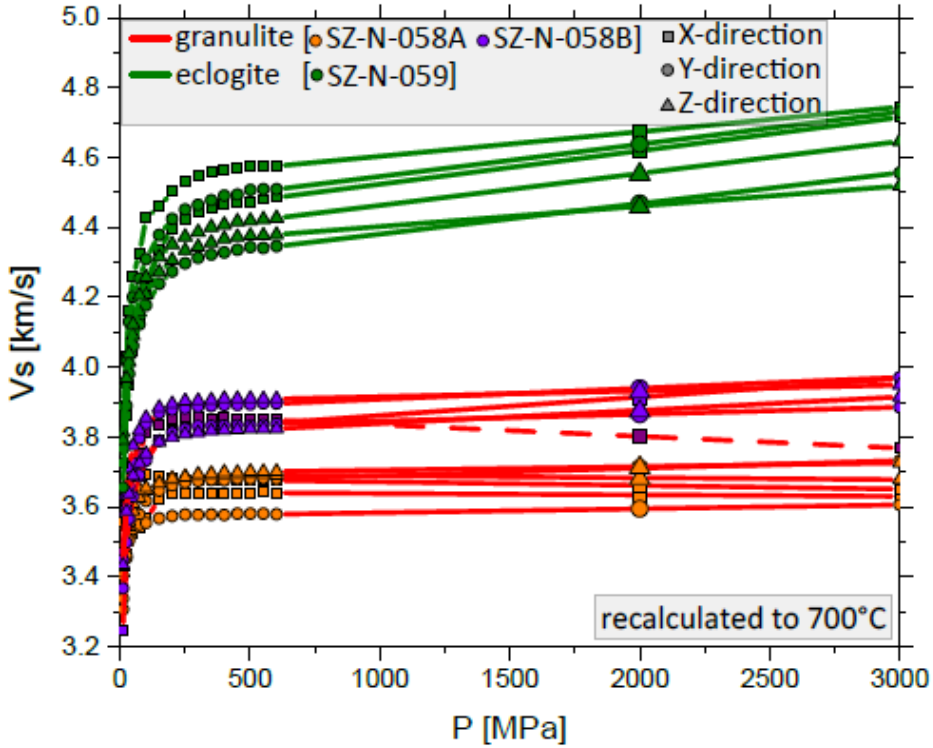

- mean Vp:
- 7.00km/s (granulite)
- 8.07 km/s (eclogite)

- mean Vs:
- 3.67 km/s (granulite)
- 4.57 km/s (eclogite)

- Anisotropy: Anis(P): $\sim$ 2 % (gran.); 10 % (eclogite)
- Anisotropy: Anis(S):$<$ 3 % (gran.); $\sim$ 4 % (eclogite)

Zertani et al., (2018)

Combining the results

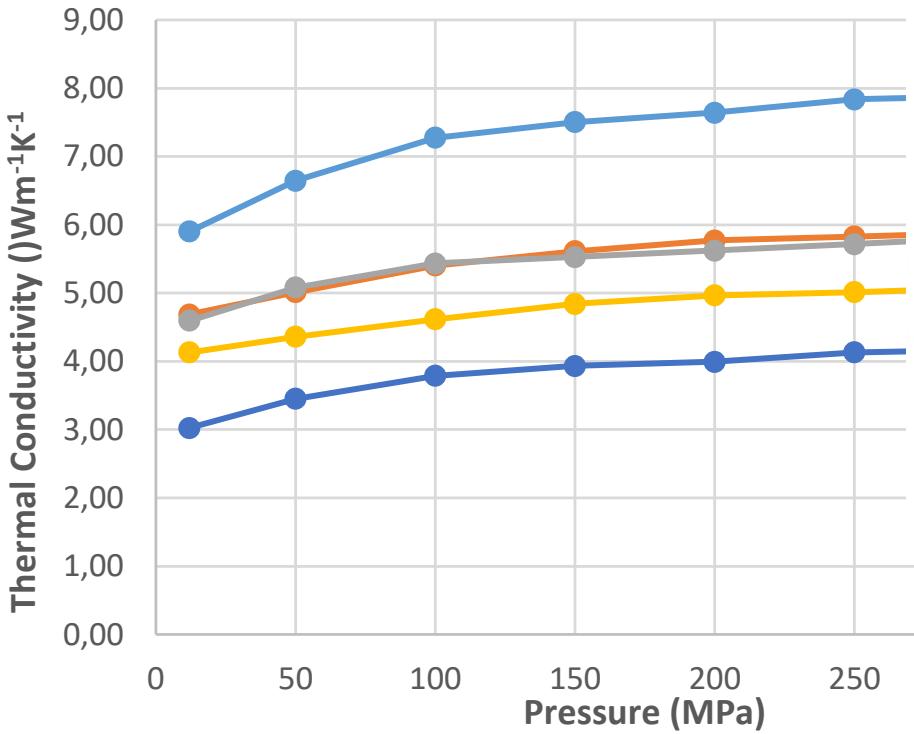

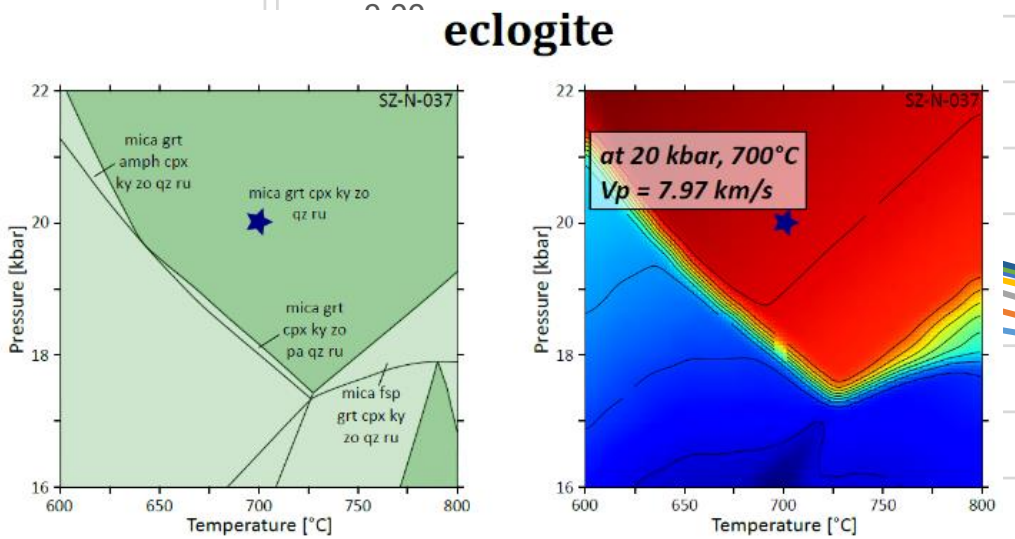

- Mean velocity for granulite: 7.18 km/s (Vp); mean velocity for eclogite: 7.98 km/s (Vp)

- Both methods provide consistent estimates of p-wave velocities
- Direct measurements additionally provide information regarding seismic anisotropy
- Thermodynamic modelling provides the opportunity to obtain velocities for a larger amount of samples

Development of the numerical toolbox

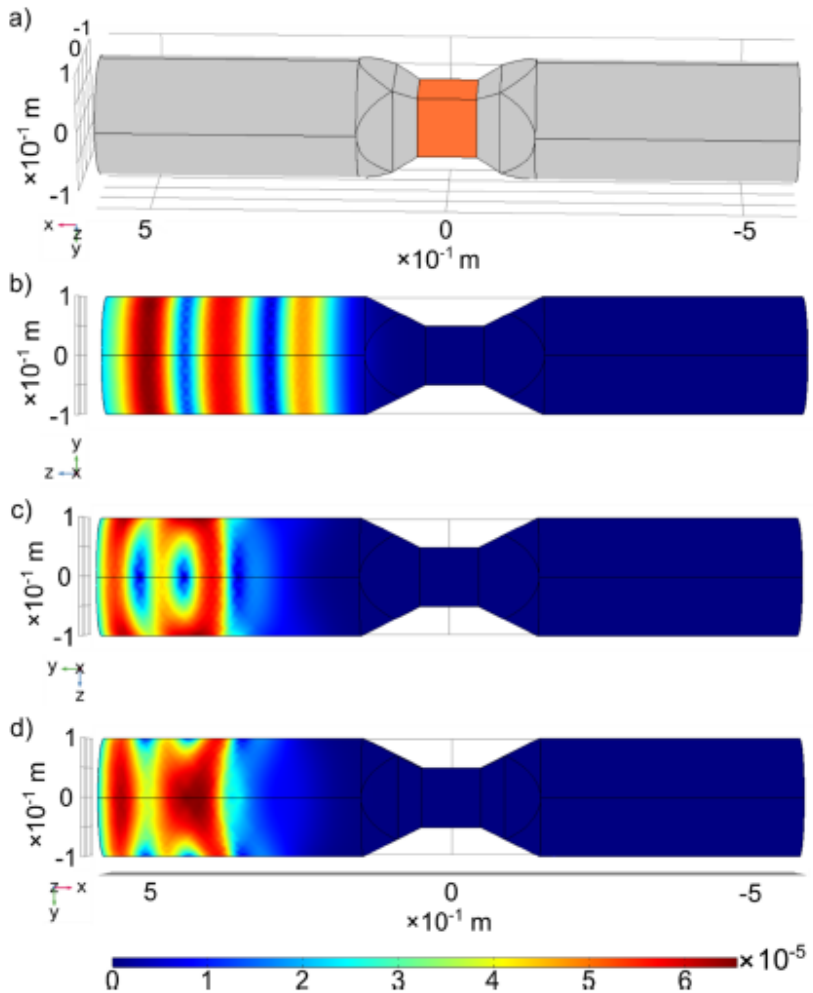

Bazargan et al., (2022)

Numerical model of three-dimensional steel specimen; the model is based on the isotropic material behavior, (a) model geometry, (b) compressional wave result, (c) shear wave with horizontal polarization, (d) shear wave vertical polarization.

Development of the numerical toolbox

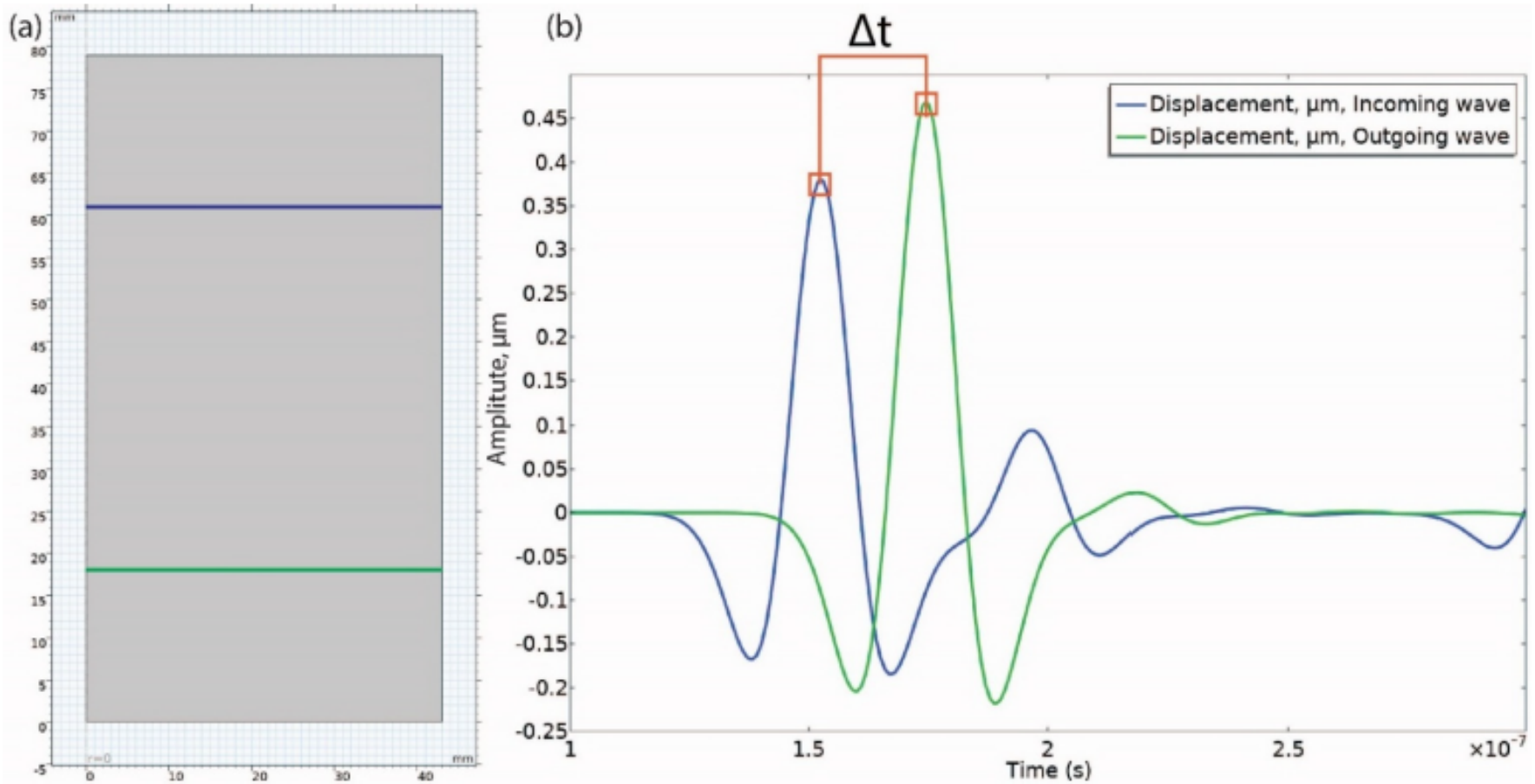

Bazargan et al., (2022)

Illustration showing how the velocity is calculated from the incoming and outgoing waves; a) geometry of investigation and the two sensor boundaries for the elastic wave (in blue and green), b) wave form, where t is the time of flight-of-flight, determined from the peak amplitudes in the two waveforms.

Development of the numerical toolbox

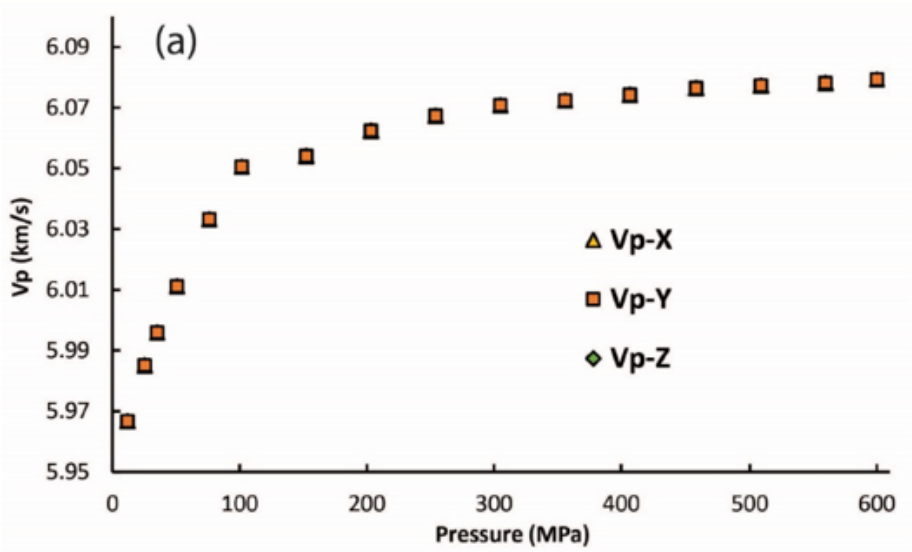

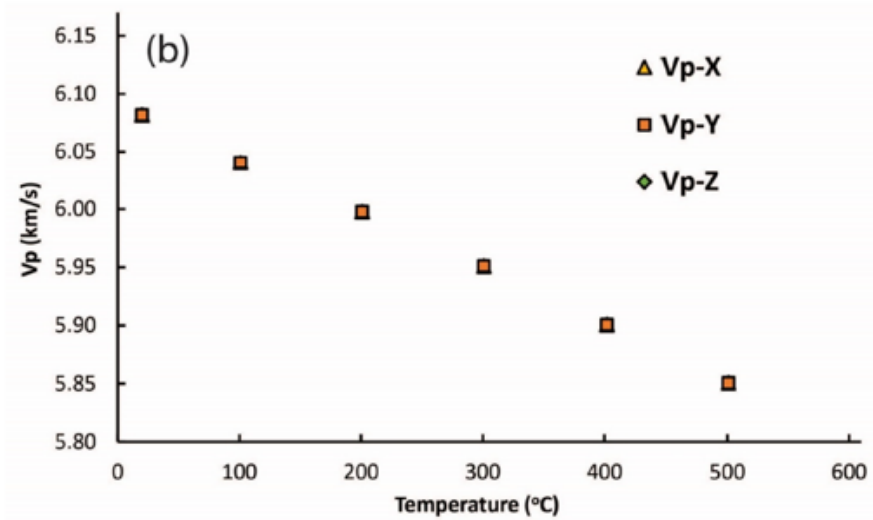

Bazargan et al., (2022)

Vp calculations from the two- and three-dimensional numerical modeling with COMSOL, investigating the effect of a) pressure and b) temperature on the elastic wave speed. Note that the models consider the changes in linear strain, dynamic elastic moduli (Young's modulus and Poisson ratio) and density. In contrast, the Vp and Vs measurements depend on the time-of-flight of the elastic wave and the change in sample length

Development of the numerical toolbox

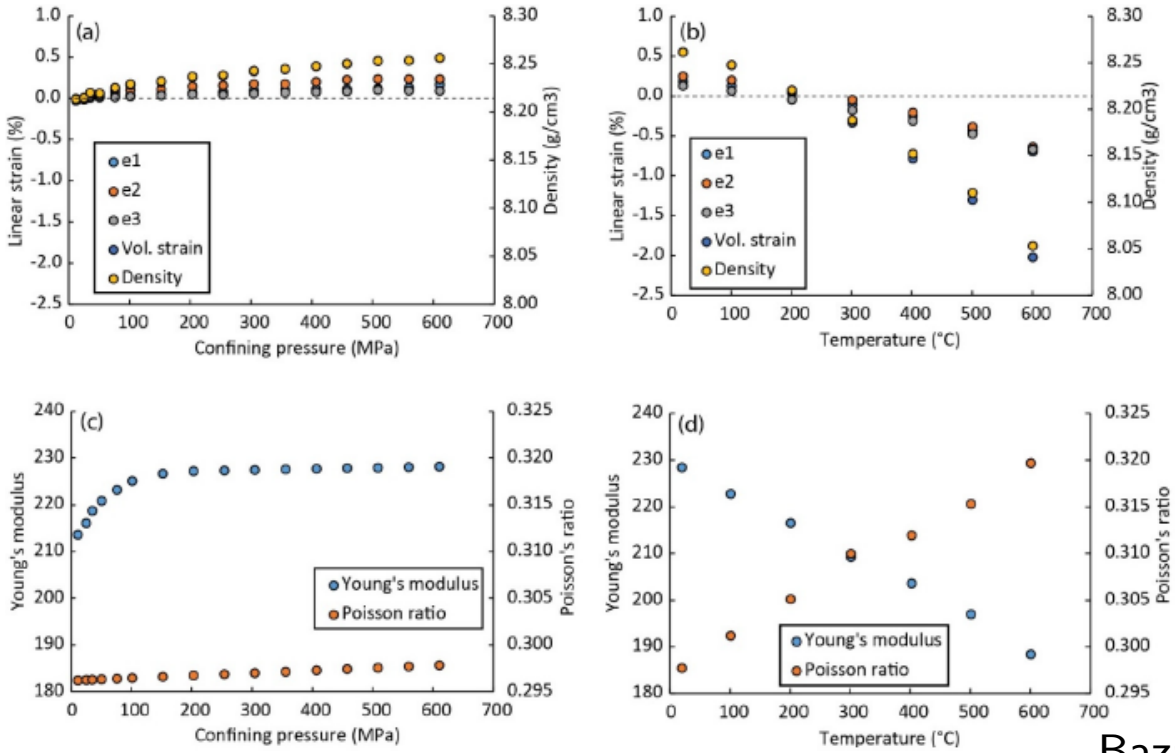

Bazargan et al., (2022)

Linear strain as a function of confining pressure, along the different sample axes (e1, e2 and e3), as well as the volumetric strain; change in density in calculated based the change in linear strain. (b) Linear strain and density as a function of temperature. (c), (d) Calculated Young's modulus and Poisson's ratio (from the mean Vp and Vs), as a function confining pressure and temperature, respectively.

Summary and conclusions (Part I)

Pressure, temperature ans mineralogical effects: elastic constants

- Elastic wave velocities and elastic constants of crustal rocks at pressure, temperature and mineralogical conditions are controlled by the state of micro-fracturing, in addition to the mineral composition and the single crystal velocities of the rock-forming minerals.
- The modal mineral composition, which is a function of both, chemical composition and metamorphic grade, may control the intrinsic velocities of crustal rocks.
- Elastic constants and petrophysical characteristic of rock can be derived from the seismic wave velocities as a function of pressure and temperature
- The multi-anvil pressure apparatus provides a unique and comprehensive experimental platform for determining seismic wave velocities, shear-wave splitting, seismic anisotropy, and the full set of elastic constants of a rock sample as functions of pressure, temperature, and mineralogical composition. Notably, this apparatus enables all these measurements to be obtained from a single sample test, ensuring consistent boundary conditions and minimizing uncertainties associated with sample-to-sample variability while capturing the coupled thermo-mechanical and compositional effects on rock elastic behavior.

Summary and conclusions (Part II)

Numerical modeling

- Seismic anisotropy and shear wave splitting, characteristics of crustal rocks and CPO of the constituent minerals and the structural frame of the rocks (foliation and lineation).
- The calculation of the physical properties from microstructural information (crystal orientation, volume fraction, grain shape etc.) is important for rocks because it gives insight into the role of microstructure in determining the bulk properties.
- Numerical modeling using COMSOL Multiphysics and thermodynamic modeling approaches are also employed to interpret seismic wave velocity measurements and to determine the elastic constants of rocks. These models explicitly account for mineralogical composition, phase proportions, and microstructural characteristics such as grain geometry, pore structure, and crack density, enabling a more realistic representation of rock elastic behavior under varying pressure and temperature conditions.

References

https://svs.gsfc.nasa.gov/30988/
https://www.internetgeography.net/topics/structure-
Schmitt, J.C.R.: Elastic anisotropy of a metamorphic rock sample of the canadian shield in northeastern alberta. RockMech. Rock. Eng. 48, 1369–1385 (2015).
Tsvankin, I., 2001. Seismic signatures and analysis of reflection data in anisotropic media. Handbook of Geophysical Exploration : SEISMIC Exploration, 1. ed. 29. Pergamon, Amsterdam U.A.
Kern, H., Liu, B., Popp, T., 1997. Relationship between anisotropy of p and swave velocities and anisotropy of attenuation in serpentinite and amphibolite. J. Geophys. Res. Solid Earth 102 (B2), 3051–3065.
Hartmut Kern, Shan Gao, Zhengmin Jin, Till Popp, Shuyan Jin: Petrophysical studies on rocks from the Dabie ultrahigh-pressure (UHP) metamorphic belt, Central China: implications for the composition and delamination of the lower crust. Tectonophysics 301 (1999) 191–215
Bazargan, M., Almqvist, B., Motra, H. B., Broumand, P., Schmiedel, T., Hieronymus, C., "Elastic Wave Propagation in a Stainless-Steel Standard and Verification of a COMSOL Multiphysics Numerical Elastic Wave Toolbox", In: Resources, 11, 49.
Kern et al. (2009), Elastic wave velocities, chemistry and modal mineralogy of crustal rocks sampled by the Outokumpu scientific drill hole: Evidence from lab measurements and modeling, Physics of the Earth and Planetary Interiors 175 (2009) 151–166
Wang et al (2005), Pressure dependence and anisotropy of P-wave velocities in ultrahigh-pressure metamorphic rocks from the Dabie–Sulu orogenic belt (China): implications for seismic properties of subducted slabs and origin of mantle reflections, Tectonophysics, 398 (2005), pp. 67-99
Motra, H. B., Magar, J., Ismail, A., Wuttke, F., Rabbel, W., Köhn, D., Thorwart, M., Simonetta, C., Costantin, N., "Determining the influence of pressure and temperature on the elastic constants of anisotropic rock samples using ultrasonic wave techniques", In: Journal of Applied Geophysics (2018a) Vol. 159, 715-730
Zertani, S., John, T., Tilmann, F.,Motra, H. B., Keppler, R., Andersen, T. B., Labrousse, L., "Modification of the seismic properties of subducting continental crust by eclogitization and deformation processes", In: Journal of Geophysical Research: Solid Earth, 124, (2019) 9731–9754. Lebesev et al. (1974), Behavior of the pore space in Granite and its relationship with elastic wave velocities and high pressure, Gerlaudes Beitr. Geophysik, Leipzig S3 (1974)2/3. S. 170-180
Gebrande et al., 1982, Elasticity and inelasticity K.-H. Hellwege (Ed.), Landolt-Brnstein. Numerical data and functional relationships in science and technology, Springer-Verlag, Berlin (1982), pp. 1-233 New Series; Group V. Geophysics and Space Research. Vol. 1b: Physical Properties of Rocks

Acknowledgment

Acknowledgment statement

The author gratefully acknowledges the support of the European Geosciences Union (EGU) through the Higher Education Teaching Material Grant 2025, which enabled the development of this teaching material.